BOLT BERANEK AND NEWMAN

FLEXURAL WAVES IN DAMPED SANDWICH PLATES

ONR Contract Nonr-(3-1(00)
Task NR 064-406

26 June 1958

Submitted to:

Mr. Philip B. Kunkel
Head, Mechanics Branch
Office of Naval Research
Washington 25, D. C.

FC

FLEXURAL VIBRATION DAMPING OF MULTIPLE-LAYER PLATES

by

Dr. Donald Ross
Dr. Edward M. Kerwin, Jr.
Dr. Ira Dyer

ONR Contract Nonr-2321(00)
Task NR 062-205

26 June 1958

BOLT BERANEK AND NEWMAN INC.
50 Moulton Street
Cambridge 38, Massachusetts

FLEXURAL VIBRATION DAMPING OF MULTIPLE-LAYER PLATES

Table of Contents

		Page
	SUMMARY	1
I.	SIGNIFICANCE OF THE PROBLEM	2
II.	ANALYSIS OF THE THREE-LAYER PLATE	4
	Assumptions	4
	Basic Equations	5
	Flexural Rigidity of Three-Layer Plate	7
	Shear Strain of the Middle Layer	10
III.	NON-CONSTRAINED DAMPING LAYERS	13
	Two-Layer Bar	13
	Damping Material on Two Sides of a Beam	15
	Practical Applications	16
IV.	CONSTRAINED DAMPING LAYERS	17
	Equations	17
	Thin Damping Tape	19
	Sandwich Plate	20
	Calculations for Constrained Damping Layers	22
V.	PROPERTIES OF VISCO-ELASTIC MATERIALS	26
	Frequency-Temperature Scaling of Elastic Properties	26
	Polyisobutylene	28
	3M Adhesive	28

REFERENCES

FIGURES

DIST. UTION LIST

FLEXURAL VIBRATION DAMPING OF MULTIPLE-LAYER PLATES

SUMMARY

In the present report the flexural vibration damping of a three-layer composite plate is analyzed for several damping configurations. When homogeneous damping layers are applied on one or both sides of the plate, the damping mechanism is associated with the alternating extensional strain of the visco-elastic damping material. The damping achieved is roughly proportional to the product of the Young's modulus and the square of the thickness of the damping layer. When a stiff layer (foil) covers the damping material, then the damping is associated with the shear motion of this material. The damping is proportional to the stiffness of the foil; but, there is an optimum thickness of the damping layer, which is a function of frequency and temperature for each material. This optimum thickness may be quite small. The theoretical relations can be used to calculate optimum damping treatments for various applications. Experimental results are in gratifying agreement with the calculated values and verify the general validity of the various physical assumptions concerning the damping mechanism.

I. SIGNIFICANCE OF THE PROBLEM

The damping of flexural vibrations in plates is becoming increasingly important as a means of noise and vibration control. Not only can damping reduce the noise radiated by vibrating plates, but also it can combat structural fatigue and equipment malfunction. The self-noise of a sonar device is often attributable to boundary-layer turbulence. In such a case, damping can be important in reducing the vibration amplitudes of the sonar enclosure. Damping is also of importance in other Navy problems dealing with sound and vibration control.

Although all elastic systems have some internal damping, this damping is usually negligible when compared to the damping that can be achieved by applying treatments making use of visco-elastic damping materials. Such treatments take several forms. A single homogeneous layer is often used, an example being automobile undercoat. A damping layer constrained by an outer layer of relatively stiff material is another promising type of damping application that is being used extensively in aircraft. Multiple applications of this "damping tape" and combinations of homogeneous layers are also used. An understanding of the mechanics of the damping of flexural vibrations is essential to the designing of optimum treatments for various applications. Since many of these damping configurations involve one or two layers applied to a basic structure, we have considered the general case of the flexural vibrations of a three-layered structure.

Historically, damping has often been treated as a somewhat mysterious phenomenon, best approached by trial-and-error methods. In recent years, Oberst[1-4]* and Liénard[5,6] have successfully analyzed the damping by single homogeneous layers of visco-elastic damping materials. They have found the damping mechanism to be associated with the stretching of the damping layer. More recently, Kerwin[7,8] has shown that the damping of a constrained layer is caused by the shear motion of the damping layer between the stiff foil and the plate. By considering the general case of a three-layer structure, we are able to derive the expressions for a single homogeneous layer and a constrained layer as special cases, while developing the general method for handling various types of damping applications involving visco-elastic damping materials.

---

*References are appended.

II. ANALYSIS OF THE THREE-LAYER PLATE

As a first step in considering the damping of practical structures, we have considered the special case of the propagation of straight-crested flexural waves in a large plate. The flexural wave motion of any shape plate can be considered as the superposition of straight-crested flexural waves. Thus, the results derived here are indicative of the damping to be expected in the more general cases of plate vibration.

Assumptions

In the most general case of a three-layered structure, the middle layer may be so soft that the coupling between the bottom and top layers is not complete, and these two layers may vibrate with different motions. In the present analysis, we assume that the middle layer is stiff enough so that the entire structure partakes of the same flexural motion. Stated another way, it is assumed that the thicknesses of the layers of the composite bar are small compared to the shortest wavelengths of any type of vibration within each layer. Specifically, the wavelength of shear waves in the damping layer must be large compared to the thickness of this layer, as these waves have the shortest wavelength.

The general approach is to find expressions for the equivalent undamped simple plate so that well-known solutions (Lord Rayleigh, Morse, Timoshenko) may be used. One then introduces internal visco-elastic damping by replacing the material properties, Young's modulus and the shear modulus, by complex quantities, both the real and imaginary terms of which are functions of the frequency and temperature. The present analysis of the three-layer plate is a

logical extension of that for a two-layer plate. The major complication in adding the third layer is the shear motion of the middle layer which now must be considered, and which actually may supply the major damping mechanism in many applications.

Basic Equations

The approximate differential equation for a plate in flexural motion is:

$$B \frac{\partial^4 z_o}{\partial x^4} + \rho A \frac{\partial^2 z_o}{\partial t^2} = 0 \qquad (1)$$

where:

z_o is the coordinate of the neutral plane

B is the flexural rigidity

ρA is the mass per unit length

In writing this equation we have omitted the corrections for rotary inertia and for the transverse shear that are usually neglected in the analysis of a thin plate. The general solution of this equation for the free motion of a finite structure having negligible damping is a combination of the various normal modes, each of which includes two "major" terms of the form:

$$e^{\pm ip_n x} e^{-i\omega_n t}$$

and two "minor" terms of the form:

$$e^{\pm p_n x} \; e^{-i\omega_n t}$$

The wave-number, p_n, and the angular frequency, ω_n, are related by:

$$B\, p_n^4 = \rho A \omega_n^2 \qquad (2)$$

For the second and higher modes, the vibration amplitudes are distributed in an essentially sinusoidal manner, and the "minor" terms may be neglected everywhere except very close to the edges. For these higher modes, the wave numbers are related to the length in the direction of the wave, L, by:

$$p_n = \left(n \pm \frac{1}{2}\right) \frac{\pi}{L} \qquad (3)$$

where the plus sign applies for free-free or clamped-clamped end conditions and the minus sign applies for one end clamped and the other end free. Substituting Eq (3) in Eq (2) and solving for the natural frequencies, one finds:

$$\omega_n = \frac{\left(n+\frac{1}{2}\right)^2 \pi^2}{L^2} \left(\frac{B}{\rho A}\right)^{1/2} \qquad (4)$$

As written above, the equations apply to undamped motions. Damping is included by replacing the various real quantities by complex quantities. The bending rigidity is a function of the elastic moduli of the materials making up the beam. If any of these moduli includes a damping factor, then that modulus will be complex and

the flexural rigidity will also be complex. The natural frequencies will then be complex, the out-of-phase component being the attenuation caused by the damping. It is assumed that the damping factor of the composite is small enough that the basic sine-wave shape of the vibrations is still valid. Eq (4) is more generally written:

$$\omega_n^* = \frac{\left(n+\frac{1}{2}\right)^2 \pi^2}{L^2} \left(\frac{B^*}{\rho A}\right)^{1/2} \qquad (5)$$

The problem of the multi-layer beam is to calculate the effective flexural rigidity and mass in terms of the dimensions and physical properties of the various layers. The mass per unit length, ρA, of the composite bar is simply the sum of the masses per unit length of the individual layers; but the effective flexural rigidity is more difficult to calculate.

Flexural Rigidity of Three-Layer Plate

The geometry of the three-layer plate is shown in Figs 1 and 2. Figure 1 represents an element in flexure, showing the shear displacement of the middle layer. The angle ϕ is the flexural angle of the element, while the angle ψ measured relative to ϕ in the opposite direction is the angle of shear of the middle layer. The neutral plane is displaced from the center of the original beam, here assumed to be layer 1*, by the addition of the damping treatment. Figure 2 presents the various thicknesses and distances used in the analysis. The displacement of the neutral plane from the neutral plane of the bottom layer is represented by D.

*This assumption does not influence the generality of the resultant equations.

Considering the three-layer element of Figures 1 and 2 we may express the bending moment M as:

$$M = B \frac{\partial \phi}{\partial x} = \sum_{1}^{3} M_{ii} + \sum_{1}^{3} F_i H_{io} \qquad (6)$$

where:

M_{ii} is the moment of the i^{th} layer about its own neutral plane

F_i is the extensional force of the layer, and

H_{io} is the height of the neutral plane of the layer above the neutral plane of the composite beam.

The various moments M_{ii} are given by:

$$M_{11} = K_1 \frac{H_1^2}{12} \frac{\partial \phi}{\partial x} \qquad (7\text{-}1)$$

$$M_{22} = K_2 \frac{H_2^2}{12} \left(\frac{\partial \phi}{\partial x} - \frac{\partial \psi}{\partial x} \right) \qquad (7\text{-}2)$$

$$M_{33} = K_3 \frac{H_3^2}{12} \frac{\partial \phi}{\partial x} \qquad (7\text{-}3)$$

where K_i is the extensional stiffness of a unit length of the i^{th} layer ($K_i = E_i A_i$) and $\frac{1}{12} H_i^2$ is the square of the radius of gyration.

Figure 3 shows the distribution of the extensional stress. This stress is proportional to the product of Young's modulus for the material and the extensional strain. The extensional force on each layer is obtained by integrating the stress for that layer:

$$F_1 = K_1 H_{10} \frac{\partial \phi}{\partial x} \tag{8-1}$$

$$F_2 = K_2 \left(H_{20} \frac{\partial \phi}{\partial x} - \frac{H_2}{2} \frac{\partial \psi}{\partial x} \right) \tag{8-2}$$

$$F_3 = K_3 \left(H_{30} \frac{\partial \phi}{\partial x} - H_2 \frac{\partial \psi}{\partial x} \right) \tag{8-3}$$

Thus, each force is the product of the stiffness of the layer and the extensional strain at the center of that layer. Each expression involves a distance from the composite neutral plane. Part of the problem is to determine the displacement D of this neutral plane relative to the neutral plane of the bottom layer. As the net x-direction force on the composite element must be zero, we can solve for D by setting the sum of the forces equal to zero.

$$0 = \sum_{1}^{3} F_i = -(K_1+K_2+K_3)\, D \frac{\partial \phi}{\partial x} + (K_2 H_{21} + K_3 H_{31}) \frac{\partial \phi}{\partial x}$$

$$- \left(\frac{K_2}{2} + K_3 \right) H_2 \frac{\partial \psi}{\partial x} \tag{9}$$

whence:

$$\psi = \frac{K_2H_{21} + K_3H_{31} - \left(\frac{K_2}{2} + K_3\right) H_2 \frac{\partial\psi}{\partial\phi}}{K_1+K_2+K_3} \qquad (10)$$

where $\left(\frac{\partial\psi}{\partial\phi}\right)$ is used to represent $\left(\frac{\partial\psi}{\partial x}/\frac{\partial\phi}{\partial x}\right)$. Written in terms of known dimensions and the displacement of the neutral plane, Eq (6) for the flexural rigidity becomes:

$$B = K_1 \frac{H_1^2}{I^2} + K_2 \frac{H_2^2}{I^2} + K_3 \frac{H_3^2}{I^2} - K_2 \frac{H_2^2}{I^2} \frac{\partial\psi}{\partial\phi} + K_1D^2$$

$$+ K_2(H_{21}-D)^2 + K_3(H_{31}-D)^2 - \left[\frac{K_2}{2} (H_{21}-D) + K_3(H_{31}-D)\right] H_2 \frac{\partial\psi}{\partial\phi} \qquad (11)$$

Before this result can be used together with Eq (10) to calculate the flexural rigidity for particular cases, a relationship between the shear angle ψ and the flexural angle ϕ is required.

Shear Strain of the Middle Layer

The shear strain of the middle layer may be calculated by considering the forces exerted on this layer by the adjacent layers. As shown in Fig 4 these are equal to the net forces on the top and bottom layers. The shear stress will be the smaller of these two almost-equal forces, which we may assume to be exerted by the top layer. Relating the strain to the stress:

$$\psi = \frac{-1}{G_2 w_2} \frac{\partial F_3}{\partial x} \tag{12}$$

where w_2 is the width of the middle layer. Because the two added layers are assumed to experience the same wave motion as the primary layer, the second derivative of the shear strain is related to the shear angle by:

$$\frac{\partial^2 \psi}{\partial x^2} = - p^2 \psi = \frac{p^2}{G_2 w_2} \frac{\partial F_3}{\partial x} \tag{13}$$

Taking the derivative of Eq (8-3) for the force on the top layer and substituting Eq (13) gives a relationship for the shear angle relative to the flexural angle:

$$H_2 \frac{\partial \psi}{\partial \phi} = H_2 \frac{(\partial^2 \psi / \partial x^2)}{(\partial^2 \phi / \partial x^2)} = \frac{H_{31} - D}{1 + \dfrac{G_2 w_2}{K_3 H_2 p^2}} \tag{14}$$

The second term in the denominator is a dimensionless shear parameter which is a function of the wave number p as well as of the shear modulus of the middle layer and the stiffness of the top layer. For the n^{th} mode, p_n is given by Eq (3). Using g as the symbol for the shear parameter*:

*Kerwin[7,8] gives a physical interpretation of the shear parameter as a measure of the ratio of the bending wavelength to the distance in which a localized shear disturbance decays.

$$S_n = \frac{\sigma_2 w_2}{K_3 H_2 p_n^2} = \frac{L^2}{H_2^2} \frac{\sigma_2 H_2}{E_3 K_3} \frac{1}{\pi^2 \left(n+\frac{1}{2}\right)^2} \tag{15}$$

Equations (10) and (14) are simultaneous equations involving D and $\frac{\partial \psi}{\partial \phi}$. They may each be written in terms of known dimensions and the shear parameter:

$$D = \frac{K_2\left(H_{21} - \frac{H_{31}}{2}\right) + g(K_2 H_{21} + K_3 H_{31})}{K_1 + \frac{K_2}{2} + g(K_1+K_2+K_3)} \tag{16}$$

$$H_2 \frac{\partial \psi}{\partial \phi} = \frac{K_1 H_{31} + K_2(H_{31}-H_{21})}{K_1 + \frac{K_2}{2} + g(K_1+K_2+K_3)} \tag{17}$$

Equations (15), (16), and (17) together with Eq (11) constitute a complete set of equations for the flexural rigidity of a three-layered plate in terms of the dimensions and physical properties of the three layers. Substitution of Eqs (16) and (17) directly into Eq (11) would result in an unwieldly algebraic equation.

The general solution is particularly unwieldly when the effect of damping is included. When the internal damping of the various layers is represented by making complex the corresponding moduli, then D and ψ become complex as well as the flexural rigidity B. The general solution may be used to obtain the damped solution for various special cases by making the assumptions appropriate to each case before combining Eqs (11), (16), and (17). Four special cases of practical interest are illustrated in Fig 5. These will be used to illustrate the use of the general solution.

III. NON-CONSTRAINED DAMPING LAYERS

Two-Layer Bar

The first case is that of the homogeneous damping layer considered by Oberst. The second layer is the visco-elastic damping layer having a complex Young's modulus. The third layer has zero thickness and stiffness. The shear parameter is infinite, and the damping mechanism is entirely independent of shear. Eq (16) for D becomes:

$$D^* = \frac{K_2^* H_{21}}{K_1 + K_2^*} = \frac{K_2^*}{K_1 + K_2^*}\left(\frac{H_1 + H_2}{2}\right) \qquad (18)$$

whence, the flexural rigidity is:

$$B^* = K_1 \frac{H_1^2}{12} + K_2^* \frac{H_2^2}{12} + \frac{K_1 K_2^*}{K_1 + K_2^*}\left(\frac{H_1 + H_2}{2}\right)^2 \qquad (19)$$

Expressing the complex quantities in terms of their real components and a loss factor:

$$B^* = B(1 - i\eta) \qquad (20\text{-}1)$$

$$K_2^* = K_2(1 - i\eta_2) \qquad (20\text{-}2)$$

and using lower-case letters to represent the various properties of the damping layer divided by the corresponding property of the original undamped plate (e.g., $b = B/B_1$, $k_2 = K_2/K_1$, etc), the final expressions are:

$$b = \frac{1 + 4k_2 + 6k_2h_2 + 4k_2h_2^2 + k_2^2h_2^2}{1 + k_2} \tag{21}$$

and

$$\frac{\eta}{\eta_2} = \left(\frac{k_2}{1 + k_2}\right)\left(\frac{3 + 6h_2 + 4h_2^2 + 2k_2h_2^2 + k_2^2h_2^2}{1 + 4k_2 + 6k_2h_2 + 4k_2h_2 + k_2^2h_2^2}\right) \tag{22}$$

where like Oberst we assume that the product of the damping factor times the stiffness of the damping layer is less than one-tenth the stiffness of the original bar ($k_2^2\eta_2^2 << 1$).

The relative damping factor for a bar with a single homogeneous layer is a function of the relative elastic modulus as well as the relative thickness of the damping layer. In Fig 6, the damping is plotted as a function of the relative thickness with the relative Young's modulus as the parameter. The curves also show an approximate square-law relation for damping as a function of thickness. It is convenient for calculation purposes to plot the ratio of η/η_2 to k_2h_2 as a function of h_2 for several typical values of the relative Young's modulus. This is done in Fig 7, where it is seen that over the range of thicknesses from 1/4 to about 3 times the thickness of the original bar, the relative damping factor is about 14 times the product of the relative stiffness and the relative thickness; i.e., $\frac{\eta}{\eta_2} \doteq 14\ k_2h_2$.

Damping Material on Two Sides of a Beam

A second example considers equal applications of damping material on both sides of a beam. Taking the thickness of each damping layer as half of the total thickness H_2 of damping material (in order to readily compare with the single-sided application of an equal amount of material), and calling the original plate "layer 1" even though it is in the middle, we obtain:

$$D^* = \frac{g^*}{1 + 2g^*} \left(H_1 + \frac{H_2}{2} \right) \tag{23}$$

where D* represents the displacement of the neutral plane of the composite relative to that of the lower damping layer. The expression for the relative shear strain of the base layer is:

$$H_1 \frac{\partial \psi^*}{\partial \phi} = \frac{D^*}{g} = \frac{H_1 + \frac{H_2}{2}}{1 + 2g^*} \tag{24}$$

If the plate is thin compared to a wavelength of the flexural vibration, and/or the stiffness of the damping layer small relative to that of the original plate, then the shear motion will be very small and the shear parameter will be very large compared to unity. The relative flexural rigidity will then be given by:

$$b = 1 + k_2(3 + 3h_2 + h_2^2) \tag{25}$$

and the relative damping by:

$$\frac{\eta}{\eta_2} = \frac{k_2(3 + 3h_2 + h_2^2)}{1 + k_2(3 + 3h_2 + h_2^2)} \tag{26}$$

Comparing Eq (26) with Eq (22), we find that the application of a given amount of damping material on one side of a plate is more effective than dividing the material and applying it equally on two sides. The two methods of application are equally effective only for very thin applications ($h_2 << 1$). For most practical thicknesses the single-sided application is at least twice as good. This result was to be expected because the effectiveness of a damping layer is proportional to the square of the thickness of the layer.

Pract. Applications

Recognizing that a high product of Young's modulus and the loss factor, and a low density, are desirable qualities in a damping material, Oberst and his co-workers in Germany[3,9] have developed a series of filled high-polymer materials with excellent damping characteristics. With these materials, damping factors as high as 0.2 are possible over a wide frequency range with layers of thickness equal to twice that of the base plate.

Experimental damping curves have agreed so well with the calculated values that damping tests are now considered to be an acceptable way of measuring the elastic properties of materials. Details are available in articles published by Brüel and Kjaer.[10]

IV. CONSTRAINED DAMPING LAYERS

When the visco-elastic layer is constrained by a stiff foil, the mechanism responsible for the major component of the damping should be the shear motion of the damping layer. A relatively thin layer may be quite effective and the requirements for optimum damping materials are quite different from those for the single layer where the damping mechanism involves the internal losses of the visco-elastic material undergoing extensional strains.

Equations

In adapting the general three-layer equations to this case, the only assumption made is that the extensional stiffness of the damping layer is small compared to that of the base. As relatively thin damping layers are customarily used, and as the material is also relatively soft, this assumption is not restrictive. With this assumption, Eq (16) for D becomes:

$$D^* = \frac{g^* K_3 H_{31}}{K_1 + g^*(K_1 + K_3)} \tag{27}$$

and Eq (17) for the relative shear strain is:

$$H_2 \frac{\partial \psi^*}{\partial \phi} = \frac{K_1 H_{31}}{K_1 + g^*(K_1 + K_3)} \tag{28}$$

When these relations are substituted into Eq (11), the resultant expression for the flexural rigidity is:

$$B^* = \frac{1}{12} K_1 H_1^2 + \frac{1}{12} K_3 H_3^2 + \frac{g^* K_1 K_3 H_{31}^2}{K_1 + g^*(K_1 + K_3)} \tag{29}$$

Expressing the complex shear modulus by:

$$G^* = G(1 - i\beta) \tag{30}$$

the shear parameter is then:

$$g^* = g(1 - i\beta) \tag{31}$$

and the resultant expressions for the real part of the flexural rigidity and for the damping factor are:

$$b = 1 + k_3 h_3^2 + \frac{12g\, k_3 h_{31}^2 \left(1 + g(1+\beta^2)(1+k_3)\right)}{1 + 2g(1+k_3) + g^2(1+\beta^2)(1+k_3)^2} \tag{32}$$

and $\frac{\eta}{\beta}$ =

$$\frac{12\, k_3 g h_{31}^2}{\left[1+k_3 h_3^2\right]\left[1+2g(1+k_3)+g^2(1+\beta^2)(1+k_3)^2\right] + 12 k_3 g h_{31}^2 \left[1+g(1+\beta^2)(1+k_3)\right]} \tag{33}$$

These expressions are considerably more complicated than those for the single layer. Although most practical applications require the retention of all of the terms, there are two special cases for

which the expressions are simpler and which still exhibit the same general features. These are thin damping tape and the sandwich of two identical stiff layers with a thin damping layer between them.

Thin Damping Tape

If the damping tape is very thin relative to the base, then k_3 is small relative to 1. The distance from the middle of the top layer to the middle of the base is then approximately half the thickness of the base. Eq (32) becomes:

$$b \cong 1 + \frac{3gk_3\left(1 + g(1+\beta^2)\right)}{1 + 2g + g^2(1+\beta^2)} \qquad (34)$$

and the equation for the damping is:

$$\frac{\eta}{\beta} = \frac{3gk_3}{1 + 2g + g^2(1+\beta^2)} \qquad (35)$$

If the damping factor of the material is less than 0.3, then the expression for the damping is simply:

$$\frac{\eta}{\beta} \cong 3k_3 \frac{g}{(1+g)^2} \qquad (36)$$

which is a very simple approximate result having most of the features of the more detailed expression.

All of the expressions for the damping factor have maxima in the vicinity of $g = 1$. Thus, for low values of the shear parameter ($g \gg 1$), it is inversely proportional to g. When β is small, the maximum occurs at $g \doteq 1$; and, for higher values of β, it occurs at somewhat lower values.

As the shear parameter is dependent on the thickness of the damping layer, it follows that there is an optimum thickness of damping material for each constrained-layer application. This is in contrast to the single-layer case, for which the damping increases with thickness of the layer. In constrained-layer damping, it is the foil stiffness that governs the maximum amount of damping obtainable. In fact, with a given foil stiffness, many damping materials can be made to yield closely similar damping factors, provided the proper thickness of each is chosen.

Sandwich Plate

A sandwich beam consists of a thin damping layer between two identical stiff plates. Taking H_1 to be the total thickness of the two stiff layers and H_2 as the thickness of the damping layer, the resultant expressions for D and ψ are:

$$D^* = \frac{g^*}{1 + 2g^*}\left(\frac{H_1}{2} + H_2\right) \tag{37}$$

$$H_2 \frac{\partial \psi^*}{\partial \phi} = \frac{1}{1 + 2g^*}\left(\frac{H_1}{2} + H_2\right) \tag{38}$$

whence the flexural rigidity is:

$$B^* = \frac{K_1}{4}\frac{H_1^2}{12} + \frac{g^*}{1 + 2g^*}\left(\frac{K_1}{2}\right)\left(\frac{H_1}{2} + H_2\right)^2 \qquad (39)$$

and the damping factor is:

$$\frac{\eta}{\beta} = \frac{\frac{3}{2}\, g\, (1 + 2h_2)^2}{\frac{1}{4} + \frac{5}{2}\, g + 4g^2(1+\beta^2) + 6gh_2(1+h_2)\left(1 + 2g(1+\beta^2)\right)} \qquad (40)$$

If the damping layer is relatively thin, then the terms involving h_2 become small and the damping factor for a sandwich plate can be approximated by:

$$\frac{\eta}{\beta} = \frac{3g}{\frac{1}{2} + 5g + 8g^2(1 + \beta^2)} \qquad (41)$$

The maximum damping obtainable with the sandwich is readily found from this equation and is plotted as a function of β in Fig 8. For most practical values of β, the maximum damping occurs when $g = 0.2$. For low values of the material loss factor, the maximum loss factor of the composite sandwich is 1/3 that of the damping material, while at higher values of β this ratio decreases.

Calculations for Constrained Damping Layers

The shear parameter defined by Eq (15) is a measure of the composite damping treatment consisting of damping laye~ and constraining foil. In making engineering calculations concerning damping tapes it is more convenient to separate the effects of the foil and of the damping layer. The foil can be characterized by its relative stiffness, $k_3 = K_3/K_1$, while the damping layer can be described by a modified shear parameter:

$$\Gamma \equiv gk_3 \equiv \frac{G_2 w_2}{K_1 H_2 p^2} \tag{42}$$

As a first approximation, the wave-number at any frequency can be assumed to be that for the original undamped motion. With this assumption, the shear parameter can be expressed as a function of frequency by:

$$\Gamma \doteq \frac{c_o}{2\pi\sqrt{12}\, f} \frac{G_2}{E_1 H_2} \frac{w_2}{w_1} \tag{43}$$

where c_o is the longitudinal velocity in the base plate. For many metals, the longitudinal velocity is close to 16,500 feet per second and the shear parameter can be calculated from:

$$\Gamma \doteq \frac{760}{f} \frac{G_2}{E_1 H_2} \frac{w_2}{w_1} \tag{44}$$

where H_2 is the thickness of the middle layer in feet.

For computation purposes, Eq (33) for the relative damping factor is best expressed in the form:

$$\frac{\eta}{\beta} \doteq \frac{12\,\Gamma\,h_{31}^2}{1 + \Gamma\left[2\left(\frac{1+k_3}{k_3}\right) + 12h_{31}^2\right] + \Gamma^2(1+\beta^2)\left(\frac{1+k_3}{k_3}\right)\left[\left(\frac{1+k_3}{k_3}\right) + 12h_{31}^2\right]} \tag{45}$$

The quantity h_{31} is the relative distance from the middle of the base bar to the middle of the top layer. It is calculated from:

$$h_{31} = \frac{1}{2}\,(1 + 2h_2 + h_3) \tag{46}$$

If the foil is assumed to be made of the same material as the plate, ther. $h_3 = k_3$ and the distance h_{31} can be expressed as:

$$h_{31} = \frac{1}{2}\,(1+k_3)\left(1 + \frac{2h_2}{1+k_3}\right) \qquad (k_3 = h_3) \tag{47}$$

If further, we assume that the thickness of the damping material is smaller than that of the foil, the damping factor becomes relatively insensitive to the exact value of h_2. It is then possible to plot the relative damping as a function of three major variables: k_3, expressing the stiffness of the foil; Γ, representing the shear properties of the damping layer; and, β, the loss factor of the damping layer. Taking typical values of k_3 (and corresponding typical values of h_2), families of curves of the damping factor as

a function of Γ have been calculated for values of β from 0.2 to 2. The specific formulas used for each value of k_3 are summarized below, where the terms are identified by the equation:

$$\frac{\eta}{\beta} = \frac{A\Gamma(1+Bh_2)}{1 + C\Gamma + D\Gamma^2(1+\beta^2)} \qquad (48)$$

k_3	A	B	C	D
.025	3.15	4.0	85.5	1820
.05	3.3	3.8	46	520
.08	3.5	3.7	31	250
.10	3.6	3.5	28	170
.15	4.0	3.4	22	108
.20	4.3	3.3	18	80
.25	4.7	3.2	17	62
.30	5.1	3.1	16	57
.33	5.3	3.0	15	51
.50	6.0	2.7	14.5	35

Figures 9, 10, and 11 are families of curves for the calculation of damping factors for three typical values of the relative foil thickness. Values of the coefficients A, B, C and D in Eq (48) can be found for values of k_3 other than those tabulated by reference to Fig 12. For applications in which E_3 does not equal E_1, similar computation techniques can be used.

Figures 9 to 11 show very similar families of curves. For low values of β, the peak of the damping curve occurs for Γ of the order of k_3, which corresponds to $g \doteq 1$. For increasing values of the material damping factor, the relative damping of the composite is unchanged at low values of Γ but is appreciably lower at high values of Γ. Consequently, the peak value shifts progressively to lower values of Γ and becomes somewhat lower in magnitude as the material loss factor β increases.

The damping calculations that are made using Figs 9 to 11 or the values of the coefficients A, B, C and D in Fig 12 are only approximate. A typical value of h_2 was assumed for each set of curves, at least insofar as h_2 enters in the denominator of the damping factor equation. However, the error introduced should be small compared to that in the material properties themselves. Actually, the major difficulty in calculating damping by viscoelastic materials is in obtaining accurate values of the dynamic shear modulus or Young's modulus and of the loss factor.

V. PROPERTIES OF VISCO-ELASTIC MATERIALS

The aim of damping calculations is to compute the loss factor of a given treatment as a function of frequency and temperature, and to be able to choose the optimum treatment for a given frequency and temperature range. To do this, the mechanical properties of the materials must be known. While the Young's and shear moduli of a metal vary only a small amount with temperature and/or frequency, these properties of a visco-elastic material are very sensitive functions of both frequency and temperature. Measurements may be available at only a few discrete points and it may be required to make damping calculations for other conditions. It is, therefore, important that we understand how to interpolate and extrapolate these data.

Frequency-Temperature Scaling of Elastic Properties

The elastic moduli of high polymers (rubberlike materials) are a function of the average chain length of the molecules between hindrances.* The longer the chain, the lower the elastic moduli. For "soft" rubberlike materials, the moduli are of the order of 10^7 dynes/cm^2, while "hard" materials have values greater than 10^{10} dynes/cm^2. The effective chain length is a function of both temperature and frequency in that there are numerous cross-links between molecules, and the breaking of these is a relaxation phenomenon. Thus, at higher temperatures the bonds are weakened and the moduli are low, while at low temperatures they are stronger and the moduli are high. Similarly, at a given temperature, low-frequency vibrations occur with a period long enough to break most of the cross bonds, while high-frequency vibrations occur too quickly and the bonds are effectively rigid.

*See Nolle, Ref 11.

Working with the concept of a relaxation spectrum for the bonds in high-polymer materials, Ferry, Williams and their associates[12-14] have found universal functions that correlate temperature and frequency effects for the elastic moduli of most simple high-polymer materials. They define reduced elastic moduli by:

$$G_o = G \frac{T_o \rho_o}{T \rho} , \quad G_o'' = G'' \frac{T_o \rho_o}{T \rho} \tag{49}$$

where ρ is the density of the material, T the temperature, and G" is the imaginary part of the complex shear modulus ($G'' = G\beta$). The subscript zero refers to an arbitrary reference temperature T_o. They get single curves of G_o and G_o'' plotted as functions of a reduced frequency:

$$f_o = f a_T \tag{50}$$

The function a_T is practically a universal function of temperature for the first 100°C above the "glass transition" temperature. Empirically,

$$\log_{10} a_T = -8.86 \frac{T - T_s}{101.6 + T - T_s} \tag{51}$$

where T_s is an empirical reference temperature for each material and is about 45°C higher than the "glass transition" temperature. Fig 13 is a plot of the logarithm of the temperature-frequency coefficient a_T as a function of $T - T_s$ in degrees Centigrade. Above 50°C, different materials follow somewhat different relaxation curves and the dashed curve represents a mean that can be used when lacking detailed data.

With the concept of temperature equivalence of frequency provided by Eqs (50) and (51), it is possible to use dynamic mechanical data taken at a moderate number of frequencies and temperatures to interpolate and extrapolate to other frequencies and temperatures. The only constant that must be found is the reference temperature T_s.

Polyisobutylene

The measurements of the dynamic shear modulus for polyisobutylene by Ferry, Grandine and Fitzgerald[15] can be used to demonstrate the effectiveness of the temperature-frequency method of correlating this type of data. Measurements covering the frequency range 40 cps to 4 kc and the temperature range -45°C to +40°C are included in Fig 14. The real part of the shear modulus and the loss factor have been plotted directly as a function of $\log_{10} fa_T$, without resorting to the correction of the dynamic modulus data to a standard temperature by means of Eq (49). The reference temperature T_s is -33°C for polyisobutylene. The range of $T-T_s$ covered by the data is -12° to +73°, extending well into the dashed portion of Fig 13. The excellent correlation of the polyisobutylene data shown in Fig 14 supports this method of handling dynamic moduli.

3M Adhesive*

The experimental configurations used by BBN to test the validity of the damping calculations have mostly used an adhesive by the Minnesota Mining and Manufacturing Company. Measurements have

*"Sound-damping-tape" adhesive, currently being used by the Minnesota Mining and Manufacturing Company in their aluminum foil tape series.

been made by this company of a sample of their adhesive at five different temperatures in the range -30°C to +60°C. An average of three valid measurements were made at each temperature, in the frequency range 30 cps to 1 kc. Assuming the same reference temperature as for polyisobutylene, these data are plotted as a function of $\log_{10} fa_T$ in Fig 15. With so few data points, it was not felt that any better correlation could be obtained by revising the choice of T_s.

Using Fig 15, values for the real part of the shear modulus and the loss factor of the 3M adhesive were determined at selected temperatures as a function of frequency. (Figs 16 and 17). Original data points are included in the figures and again show that the smoothed curves based on Fig 15 are a valid representation of the data. All of the calculated curves to be presented below in the section on experimental confirmation are based on the data in these two charts.

VI. EXPERIMENTAL CONFIRMATION

The general theory for the three-layer plate can be checked by experiments on the various configurations that are covered as special cases. Tests of the single homogeneous layer are reported in the literature[1-6]. The case of constrained damping is more general, because it includes the shear motion of the middle layer. It is also the more interesting because of the relative newness of the theory. In this section we report on the comparison between experimental and calculated damping factors for a set of constrained-layer configurations prepared at BBN and tested both by BBN and by Convair Division (San Diego) of the General Dynamics Corporation. The measurements reported here were all obtained as part of a Convair-sponsored investigation of damping materials.

Experimental Method

There are several methods of measuring the loss factor η of a damping configuration[10]. The method adopted is the resonance method, useful over a broad range of damping factors in the middle ground between very low and very high damping. In this method, the sharpness of a resonance is measured. The sharpness of resonance is determined by the frequency interval Δf between the two half-power points on each side of the resonance frequency f_o. The damping factor is the inverse of the "Q" of the resonance:

$$\eta = \frac{1}{Q} = \frac{\Delta f}{f_o} \qquad (52)$$

The method involves measuring the sharpness of the separate resonances, and accurate results are only possible when the separation of the resonances is at least twice their bandwidths. The flexural

resonances of bars have wider frequency separations than do those of similar-size plates. For this reason, measurements are made on bars whose widths are small compared to a wavelength instead of on plates.

The experimental apparatus used for resonance measurements is shown schematically in Fig 18. The test bar is suspended vertically with upright piano wires attached to small screws in the edges of the bar two inches from the top of the bar. It is driven near the lower end by means of a small loudspeaker voice coil cemented to the bar and a loudspeaker magnetic structure that does not touch the bar. A capacitive pickup located near the upper end senses the motion. As the oscillator frequency is varied around a given resonance, the bandwidth and center frequency are determined by the monitoring instruments. The loss factor is calculated from Eq (52). Although the damping factor is determined at a series of discrete frequencies, the results are described as a continuous function of frequency.

The measurements reported here were all made with aluminum test bars 36 inches long, 2 inches wide, and 1/8-inch thick. These bars have 17 resonances in the frequency range below 3 kc, the lowest being at 20 cps. The resonance frequencies are given closely by

$$f_n \doteq 2.25\,(2n+1)^2 \qquad n = 1, 2, \ldots \qquad (53)$$

Interspersed among the flexural resonances are torsional resonances that are not effectively damped by the damping material. The suspension wires are about 4 ft long, and the fact that very low values of η (well below 10^{-3}) are measured for undamped bars indicates that the suspension has negligible effect on the behavior of the damped bars.

The nine test bars were made up including all possible combinations of three thicknesses of 3M adhesive and three foil thicknesses. (See Table I). The damping treatments, and their corresponding dimensionless thicknesses are listed in the table. Room temperature measurements were made at BBN and the bars were then shipped to Convair, where measurements were made at a variety of temperatures from close to -30°C to room temperature. The two sets of room-temperature measurements show reasonable agreement.

Results at Room Temperature

Figures 19 and 20 present the measured and calculated loss factors for six of the test bars at room temperature. The solid curves are the calculated values, and the broken curves represent measured values. Data for Bars Q, R, and S are given in Fig 19, while Fig 20 presents corresponding data for Bars W, X, and Y. These sets of bars differ only in that the damping layer for Bars W, X, and Y is four times as thick (0.010 in.) as that for Bars Q, R, and S (0.0025 in.). See Table I.

The measured data agree quite well with the calculated curves. The general shape of the measured curves, as well as the spacing between the curves, is as expected. The theory predicts that the general damping curve for a constrained damping layer will have a broad maximum as a function of frequency. We see that at room temperature, Bars Q, R, and S provide damping at the peak of this broad maximum. The thicker damping layer used on Bars W, X, and Y reduces the shear parameter, g, enough to place the damping of these bars on the high-frequency side of the peak of the damping curve. The curves for these bars, then, slope downward with increasing frequency. It is interesting to note that a constrained damping layer can provide a damping curve that either rises, falls, or is relatively flat with frequency.

TABLE I

Dimensions of Test Bars

Thicknesses

Bar	Adhesive	Foil	h_2	$h_3 = k_3$	$2h_{31}$
Q	.0025 (in.)	.006 (in.)	.02	.048	1.09
R	"	.010	"	.08	1.12
S	"	.020	"	.16	1.20
T	.005	.006	.04	.048	1.13
U	"	.010	"	.08	1.16
V	"	.020	"	.16	1.24
W	.010	.006	.08	.048	1.21
X	"	.010	"	.08	1.24
Y	"	.020	"	.16	1.32

Results at Low Temperatures

Low temperature data on the same six bars appear in Figs 21, 22, and 23. As before, the calculated curves are shown as solid curves. Figures 21 and 22, for a temperature of -6°C, make an interesting contrast to Figs 19 and 20, the room temperature curves. At this lower temperature, the damping material has become stiffer, resulting in higher values of the shear parameter, g. The effect of this change is to shift the curves toward the left on the general damping curve. As a result, the data for Bars Q, R, and S (Fig 21) are now on the upward-sloping part of the curve, and the data for Bars W, X, and Y are nearly at the peak of the curve.

Data for Bars W, X, and Y at -27.5°C appear in Fig 23. Here we see a further shift toward the left on the general damping curve, and consequently the curves for the individual bars rise more steeply with increasing frequency.

We note that the agreement between theory and experiment is less good at the lower temperatures than at room temperature. The shape of the curves remains approximately as calculated. However, the spacing between curves is greater than the calculated spacing, showing lower measured damping factors for the bars with thinner constraining layers (Bars Q, and W). The disagreement becomes serious for the data at -27.5°C in Fig 23.

Conclusions

In comparing the theoretical and experimental values of damping factor for the test bars shown in Figs 19 to 23, we may draw several conclusions:

a) The general shape, as a function of frequency, of the experimental damping curves is as predicted by the theory. A broad maximum is observed, and the portion of this broad curve lying in a given frequency range depends on the value of the shear parameter g for the system under test.

b) The general frequency-temperature-equivalence hypothesis is borne out by the data taken at low temperatures. The shift in position on a broad, general damping curve that results from a change in temperature is seen to be equivalent to that which would be expected from an appropriate shift in frequency.

c) For the particular damping material used in the tests reported here, the agreement between theory and experiment deteriorates as temperature is reduced significantly below room temperature. However, this does not appear to be the result of a flaw in the theory, but rather may result from a discrepancy in the low-temperature dynamic properties of the damping material from batch

to batch. That is, the damping material used in the experiment was undoubtedly from a different batch than that for which the material properties were measured. Significant differences in properties can exist between batches of high-polymer materials that are supposedly prepared in the same manner. These differences would be more serious at low temperature.

Our general conclusion is, then, that the theory for the general three-layer bar, as specialized to the case of a constrained damping layer, adequately explains observed phenomena. Furthermore, this theory allows the calculation and scaling of the damping by simple constrained damping layers, and establishes procedures that may be used to analyze multiple constrained damping layer applications.

REFERENCES

1. H. Oberst, "Über die Dämpfung der Biegeschwingungen dünner Bleche durch fest haftende Beläge", Acustica, 2, Akustische Beihefte, 4, 181-194 (1952).

2. H. Oberst and G. W. Becker, "Über die Dämpfung der Biegeschwingungen dünner Bleche durch fest haftende Beläge II", Acustica, 4, Akustische Beihefte, 1, 433-444 (1954).

3. H. Oberst, "Werkstoffe mit extrem hoher innerer Dämpfung", Acustica, 6, Akustische Beihefte, 1, 144-153 (1956).

4. H. Oberst, "Akustische Anwendung von Schaumstoffen", Kunststoffe, 46-5, 190-194 (1956).

5. P. Liénard, "Etude d'une Méthode de Mesure du Frottement Intérieur de Revêtements Plastiques Travaillant en Flexion", La Recherche Aéronautique, 20, 11-22 (1951).

6. P. Liénard, "Les Mesures d'Amortissement dan les Matériaux Plastiques ou Fibreux", Annales des Télécommunications, 12-10, 359-366 (1957).

7. E. M. Kerwin, "Vibration Damping by a Constrained Damping Layer", BBN Report No. 547, 29 April 1958, submitted to Convair, San Diego.

8. E. M. Kerwin, "Vibration Damping by a Stiffened Damping Layer", Paper U-8, 55th Meeting of the Acoustical Society of America, 10 May 1958.

9. G. W. Becker and H. Oberst, "Über das dynamisch-elastische Verhalten linearer, vernetzter und gefüllter Kunststoffe", Kolloid Zeitschrift, 148, 6-16 (1956).

10. A. Schlägel, "Measurements of the Dynamic Modulus of Elasticity and the Loss Factor for Solid Materials, Parts 1 and 2", Brüel and Kjaer Technical Review, 4, (1957), 1 (1958).

11. A. W. Nolle, "Dynamic Mechanical Properties of Rubberlike Materials", Journal of Polymer Sciences, 5, 1-54 (1949).

12. J. D. Ferry, E. R. Fitzgerald, L. D. Grandine, Jr., M. L. Williams, "Temperature Dependence of Dynamic Properties of Elastomers; Relaxation Distributions" Industrial and Engineering Chemistry, 44, 703-6 (1952).

13. M. L. Williams, R. F. Landel, J. D. Ferry, "The Temperature Dependence of Relaxation Mechanisms in Amorphous Polymers and Other Glass-forming Liquids", Journal of the American Chemical Society, 77, 3701-7 (1955).

14. J. D. Ferry, L. D. Grandine, Jr., E. R. Fitzgerald, "The Relaxation Distribution Function of Polyisobutylene in the Transition from Rubber-like to Class-like Behavior", Journal of Applied Physics, 24, 911-16 (1953).

15. E. R. Fitzgerald, L. D. Grandine, Jr., J. D. Ferry, "Dynamic Mechanical Properties of Polyisobutylene", Journal of Applied Physics, 24, 650-5 (1953).

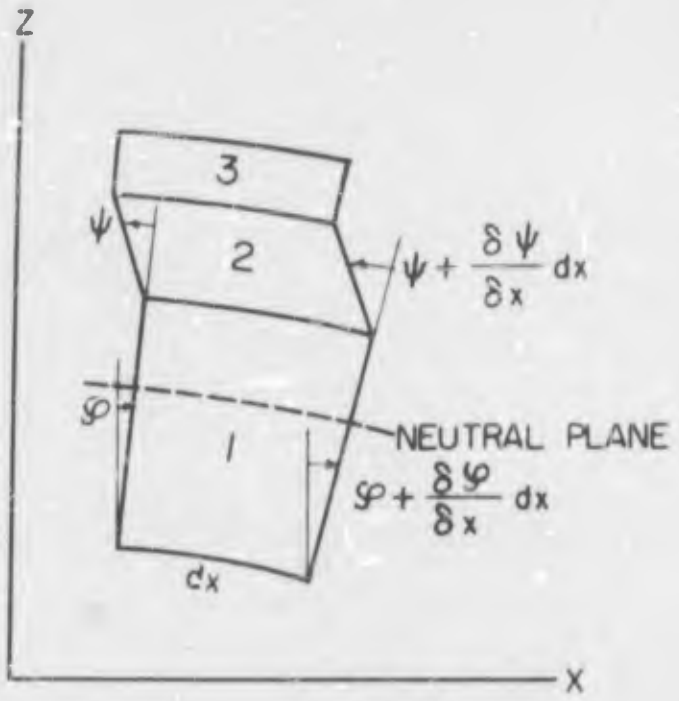

FIG. 1 ELEMENT OF A THREE-LAYER PLATE IN FLEXURAL VIBRATION, SHOWING THE FLEXURAL ANGLE φ AND SHEAR ANGLE ψ.

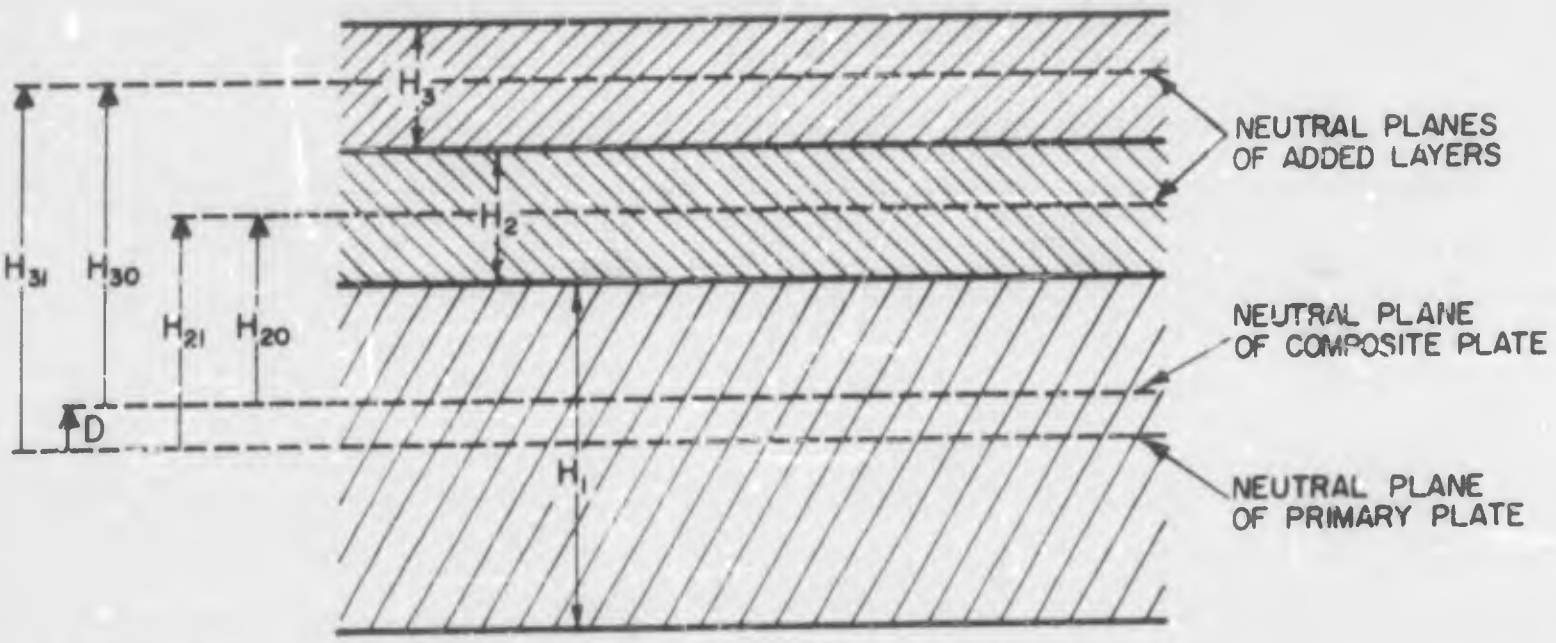

FIG. 2 DIMENSIONS USED IN ANALYSIS OF A THREE-LAYER PLATE IN FLEXURE.

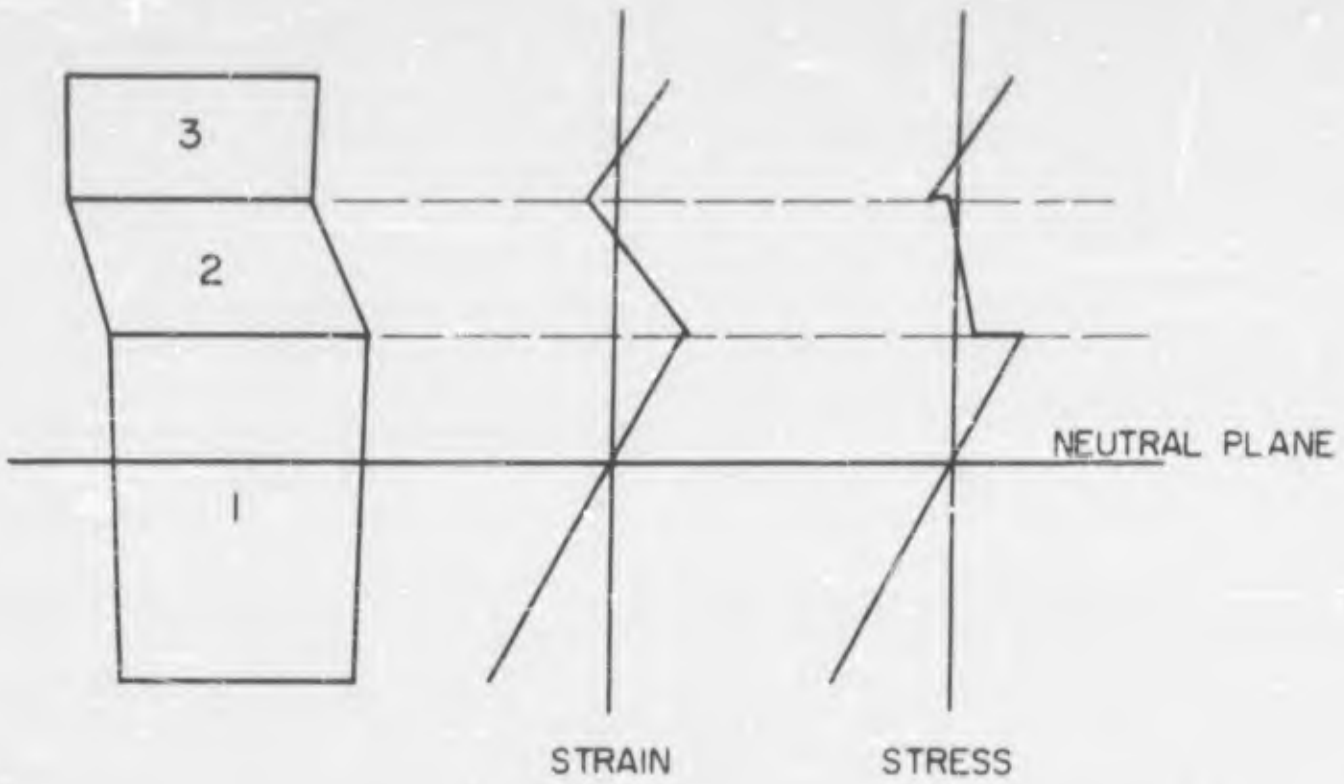

FIG. 3 EXTENSIONAL STRAIN AND STRESS DISTRIBUTIONS FOR THREE-LAYER PLATE ELEMENT IN FLEXURE.

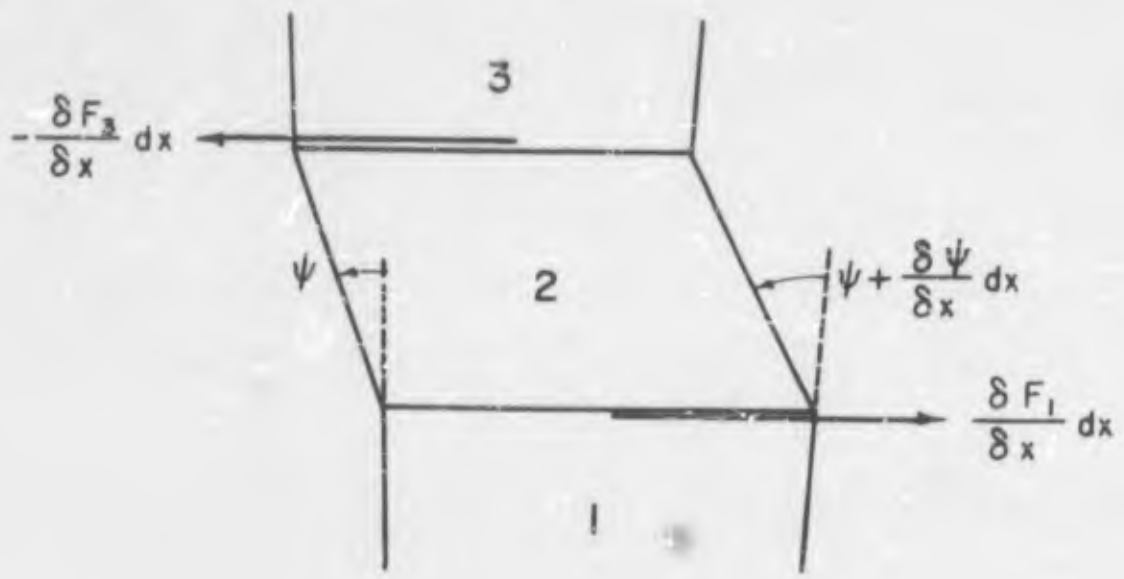

FIG. 4 SHEAR FORCE ON MIDDLE LAYER.

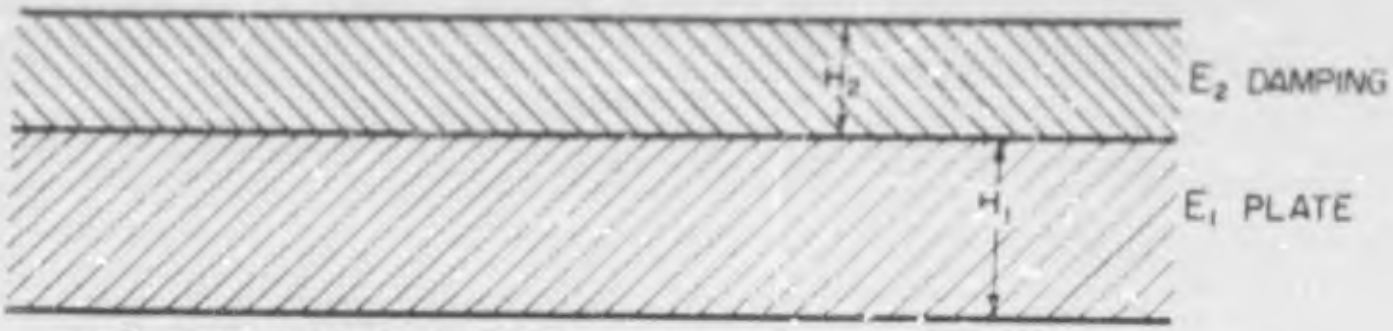

a.) TWO-LAYER PLATE

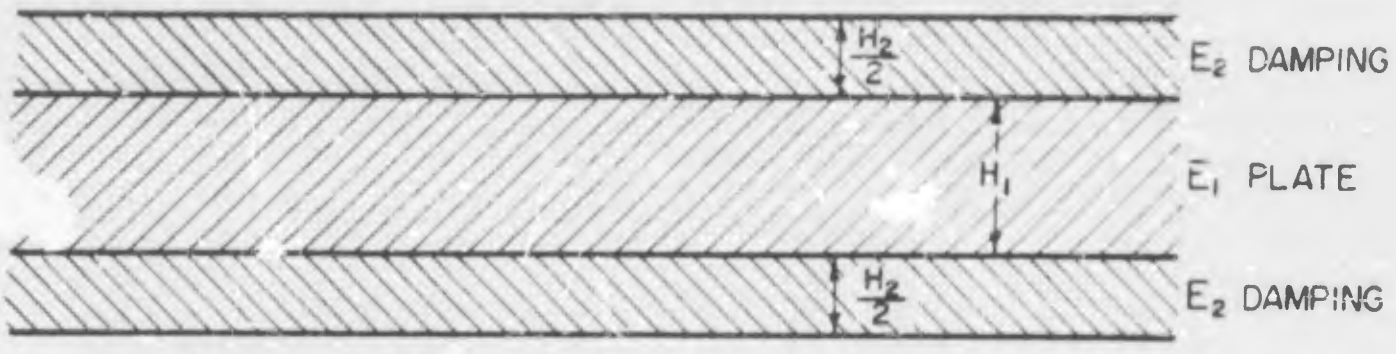

b.) EQUAL DAMPING LAYERS ON BOTH SIDES

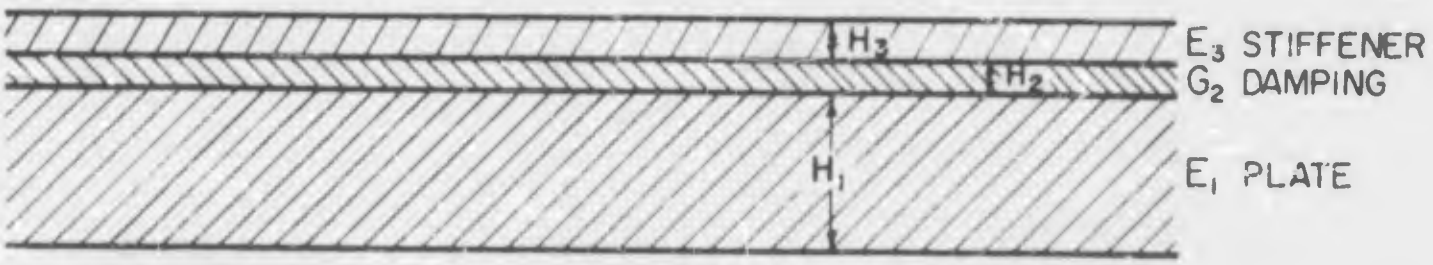

c.) DAMPING TAPE (THIN LAYERS)

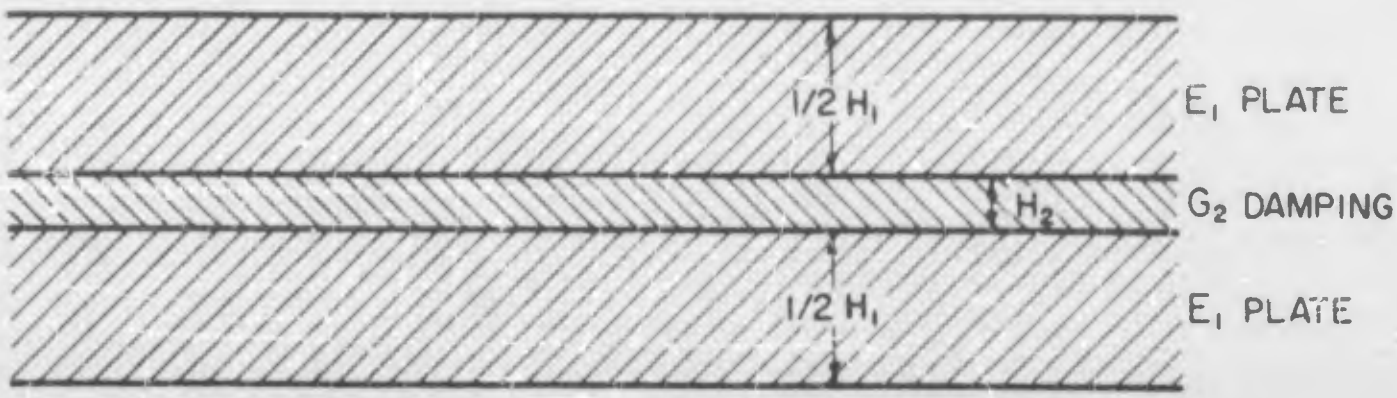

d.) SANDWICH

FIG. 5 SPECIAL CASES OF THREE-LAYER PLATES.

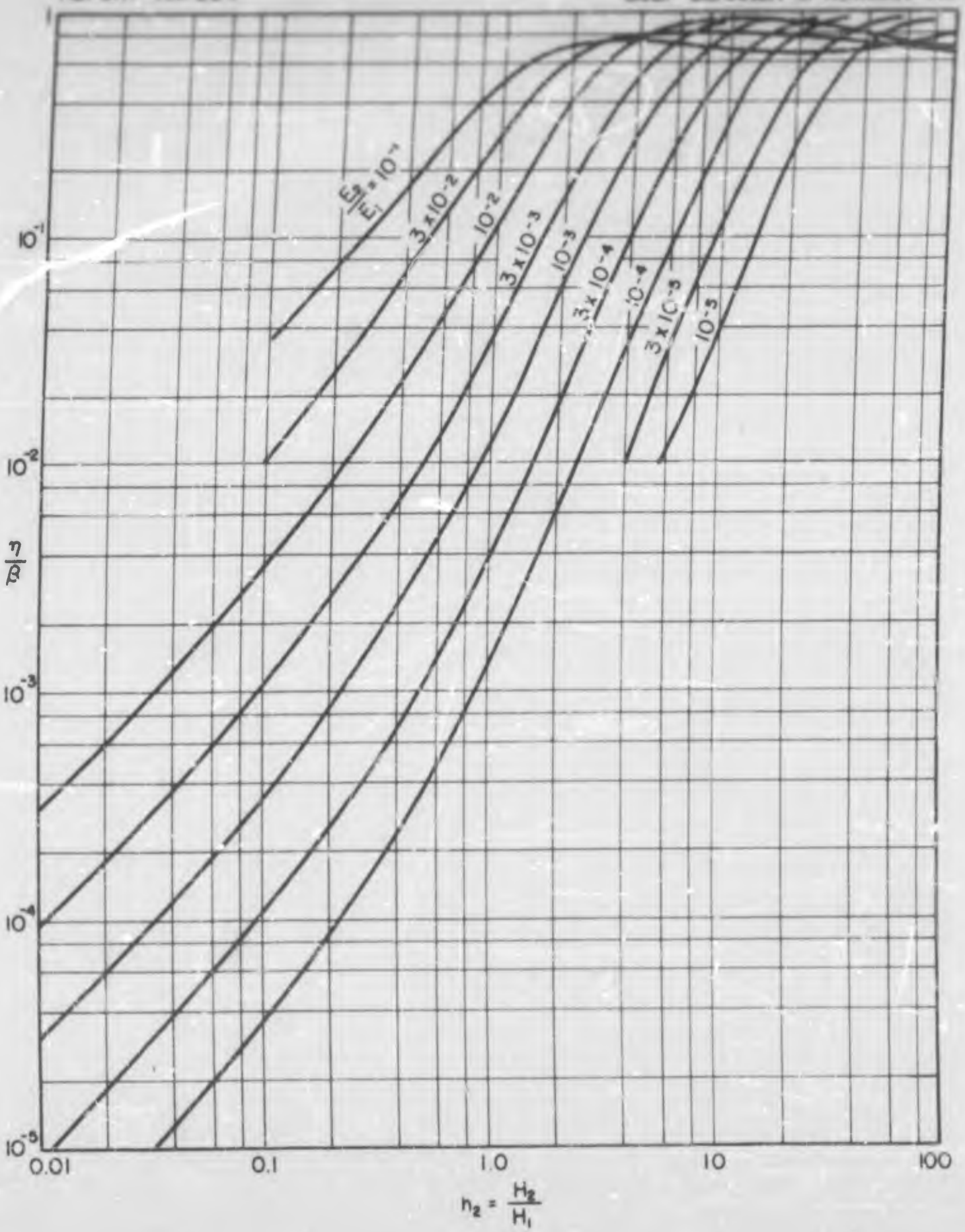

FIG. 6 RELATIVE DAMPING FACTOR FOR HOMOGENEOUS DAMPING TREATMENTS (FROM OBERST, REF. 1)

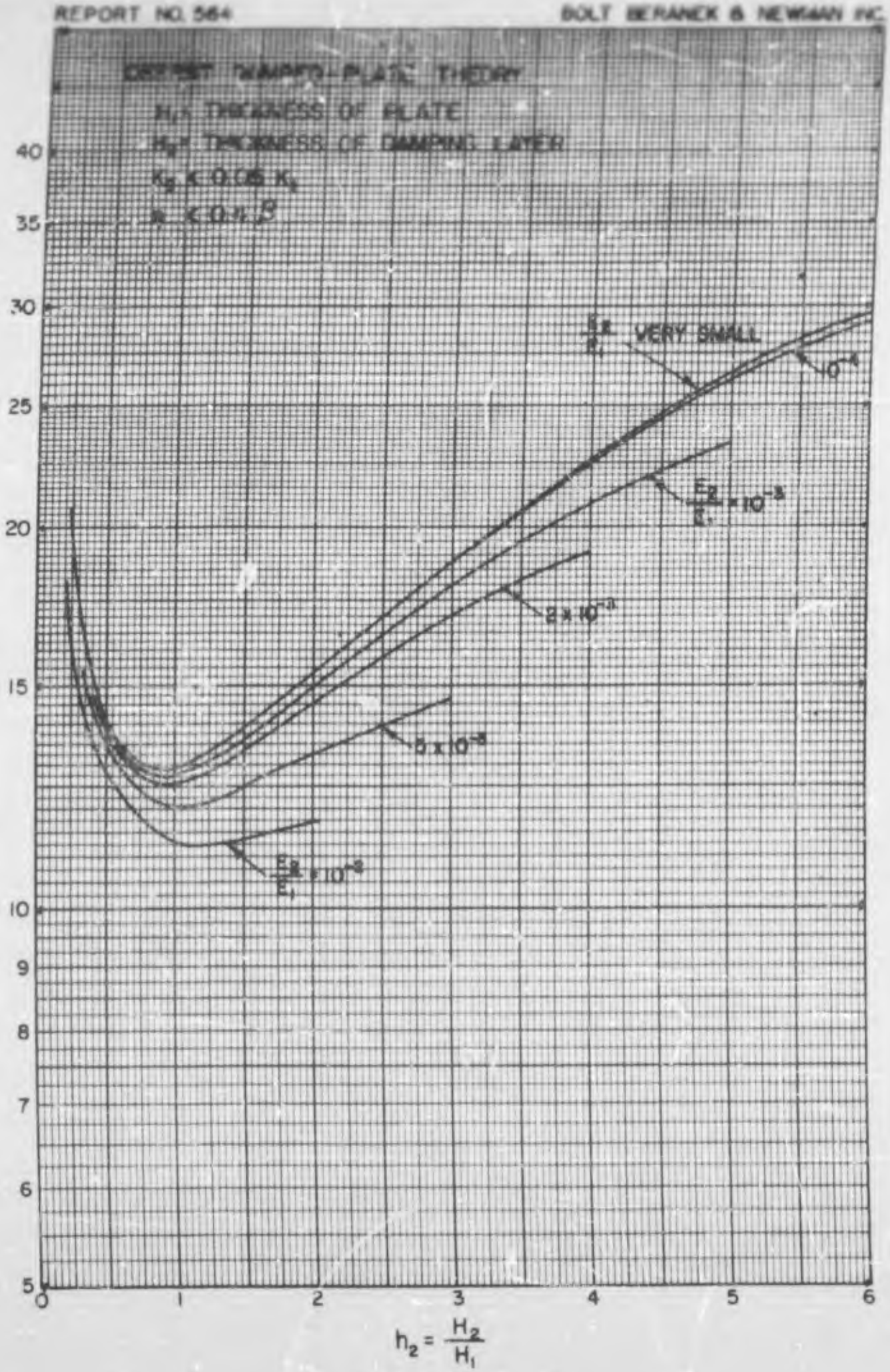
DEEPEST WAVED-PLATE THEORY
H_1: THICKNESS OF PLATE
H_2: THICKNESS OF DAMPING LAYER
$K_2 < 0.05\, K_1$
$\alpha < 0.1\, \beta$
$\frac{\eta/\beta}{K_2 H_2 / K_1 H_1}$
$\frac{E_2}{E_1}$ VERY SMALL
10^{-4}
$\frac{E_2}{E_1} \times 10^{-3}$
2×10^{-2}
5×10^{-2}
$\frac{E_2}{E_1} \times 10^{-2}$
40
35
30
25
20
15
10
9
8
7
6
5
0
1
2
3
4
5
6
$h_2 = \frac{H_2}{H_1}$

FIGURE 7

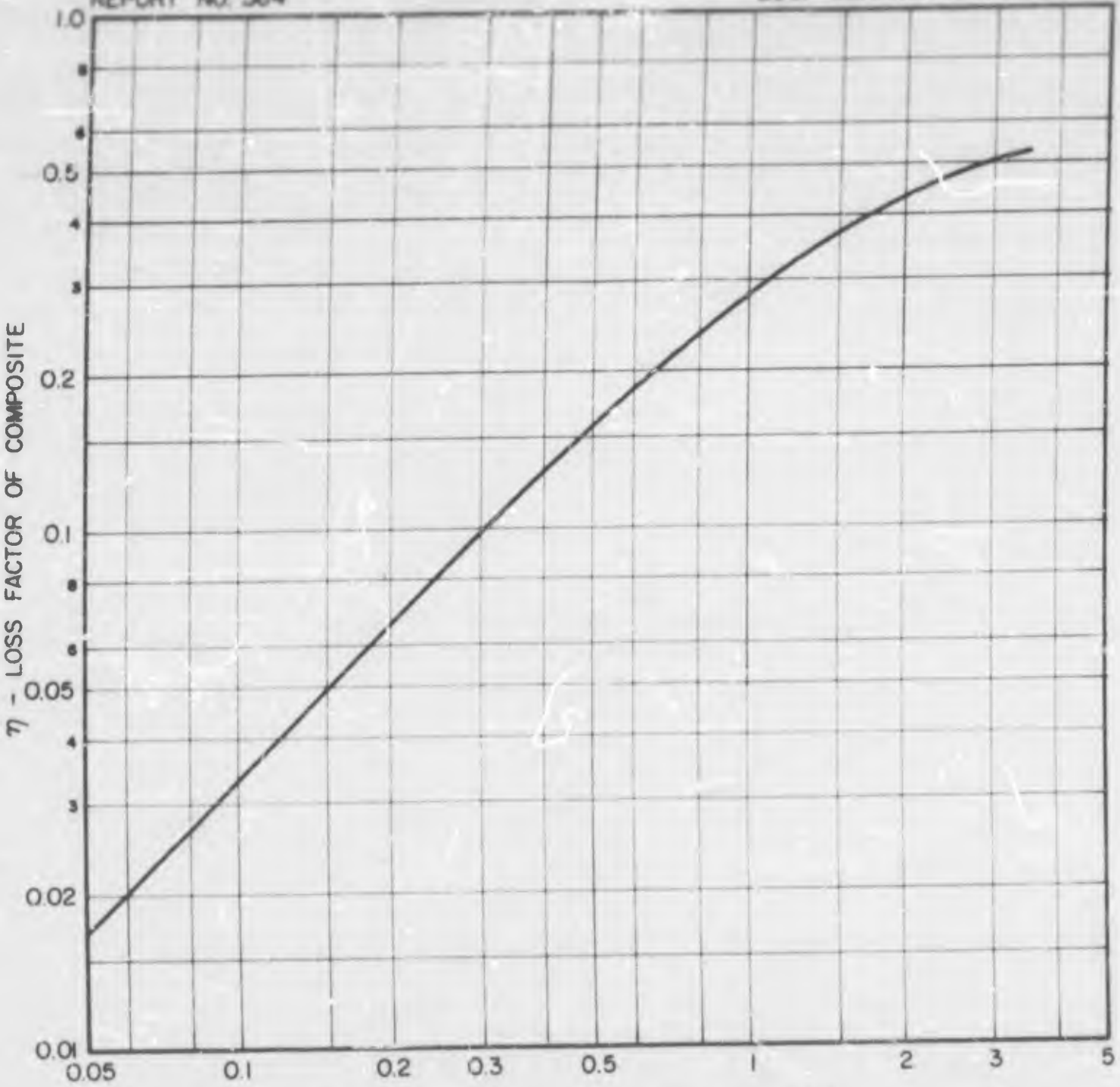

FIG. 8 MAXIMUM DAMPING OF SANDWICH STRUCTURES HAVING THIN DAMPING LAYER.

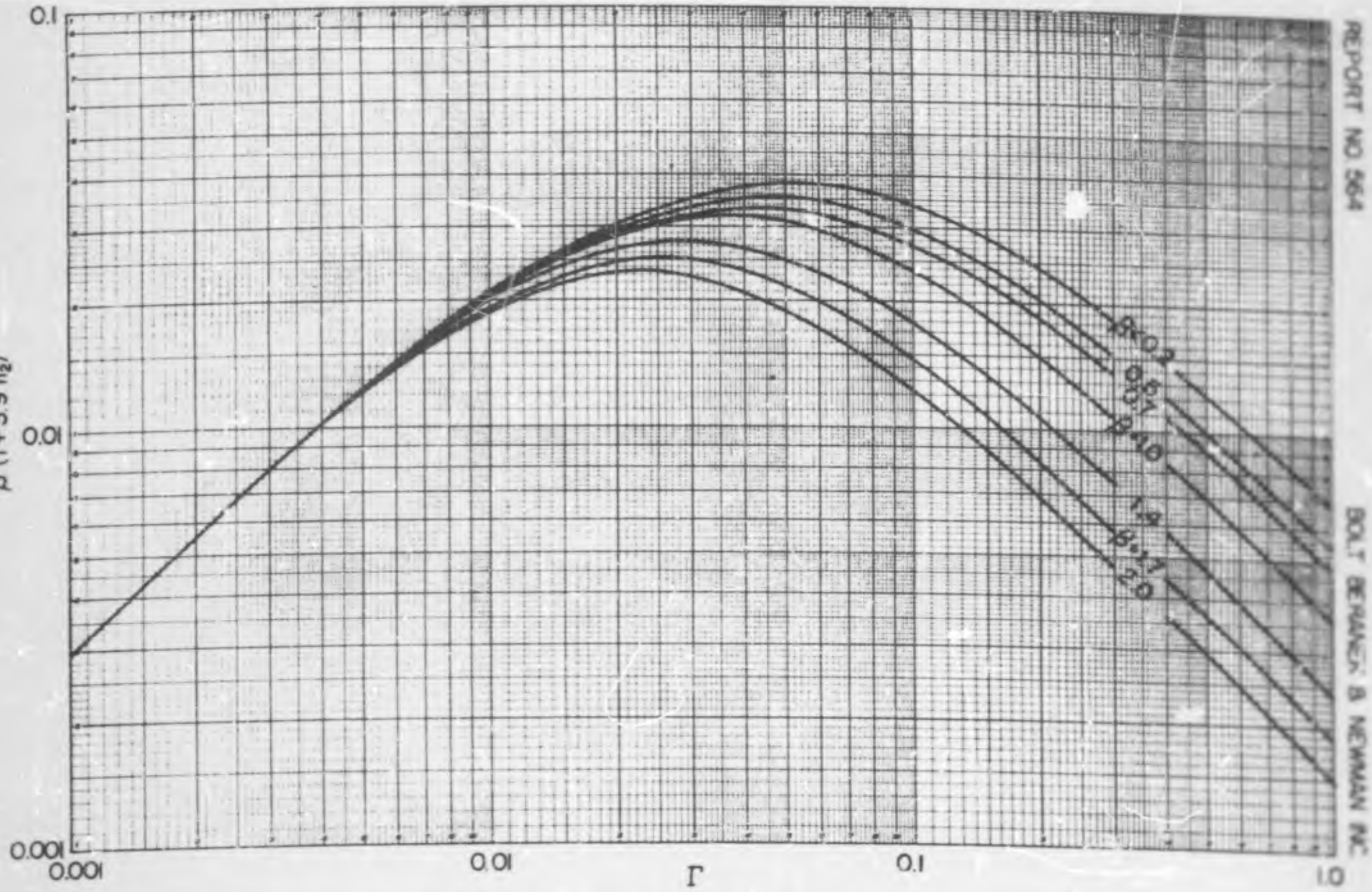

FIG. 9 DAMPING TAPE CALCULATIONS FOR $h_3 = 0.05$

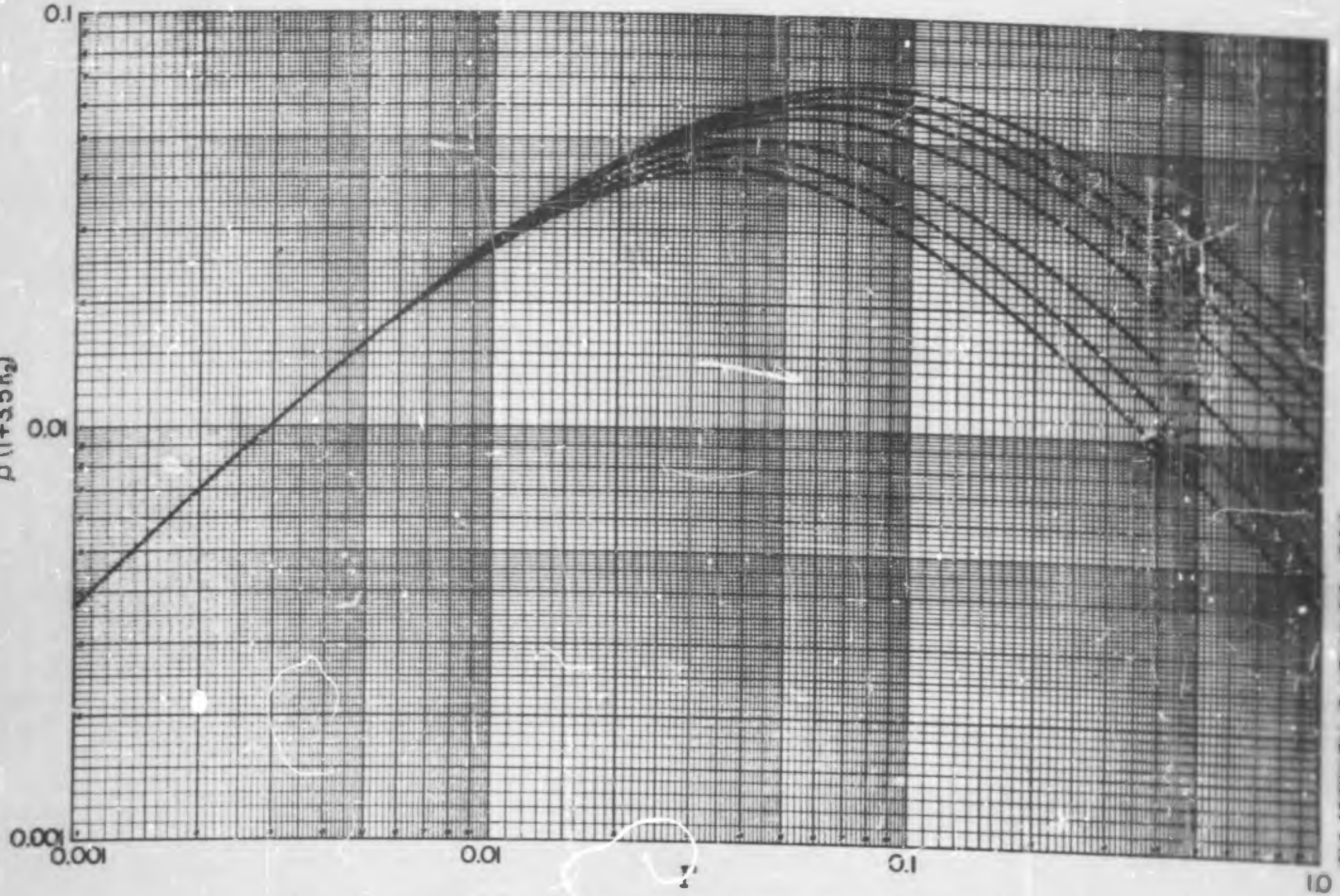

FIG. 10 DAMPING TAPE CALCULATIONS FOR $h_3 = 0.10$

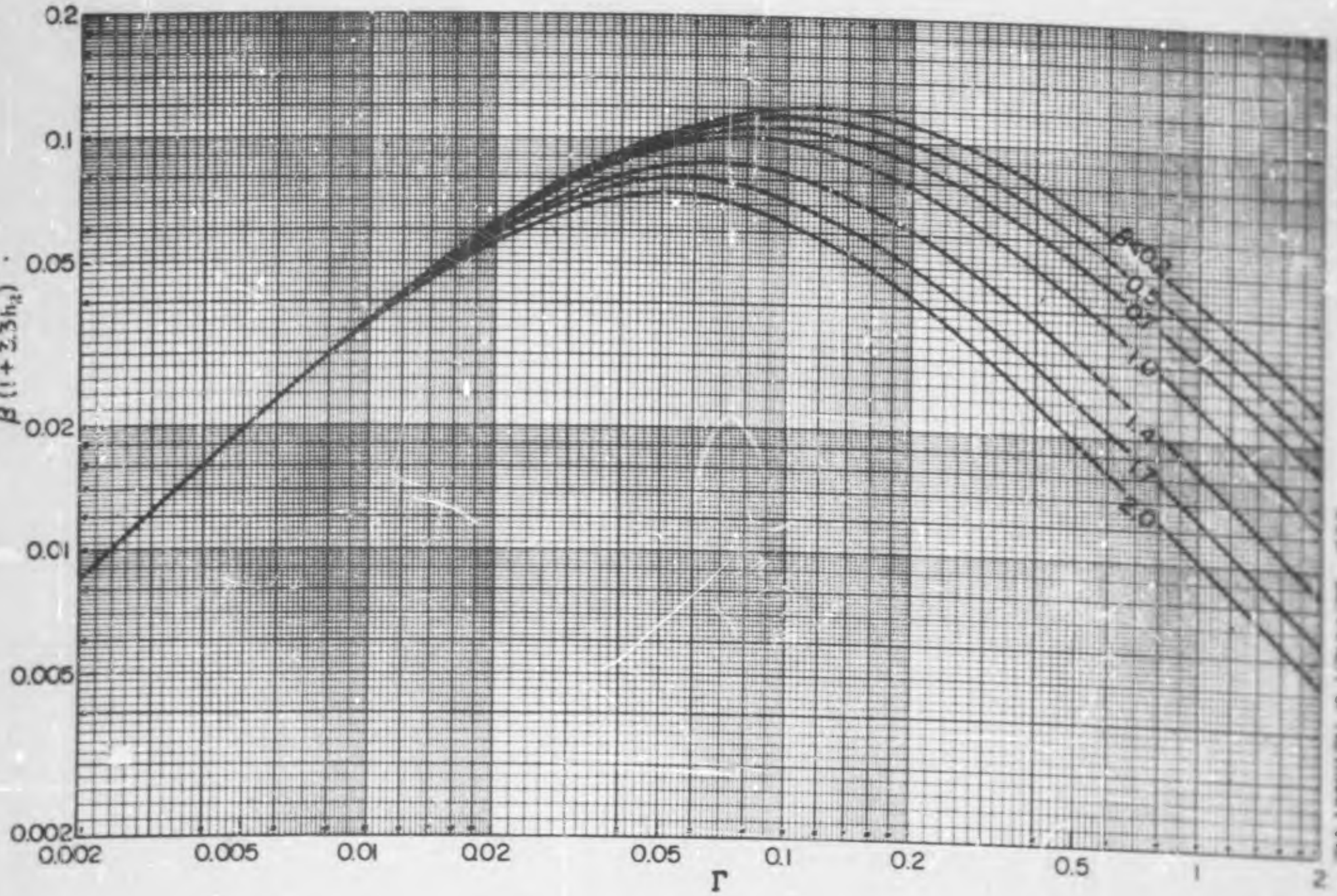

FIG. II DAMPING TAPE CALCULATIONS FOR $h_3 = 0.20$

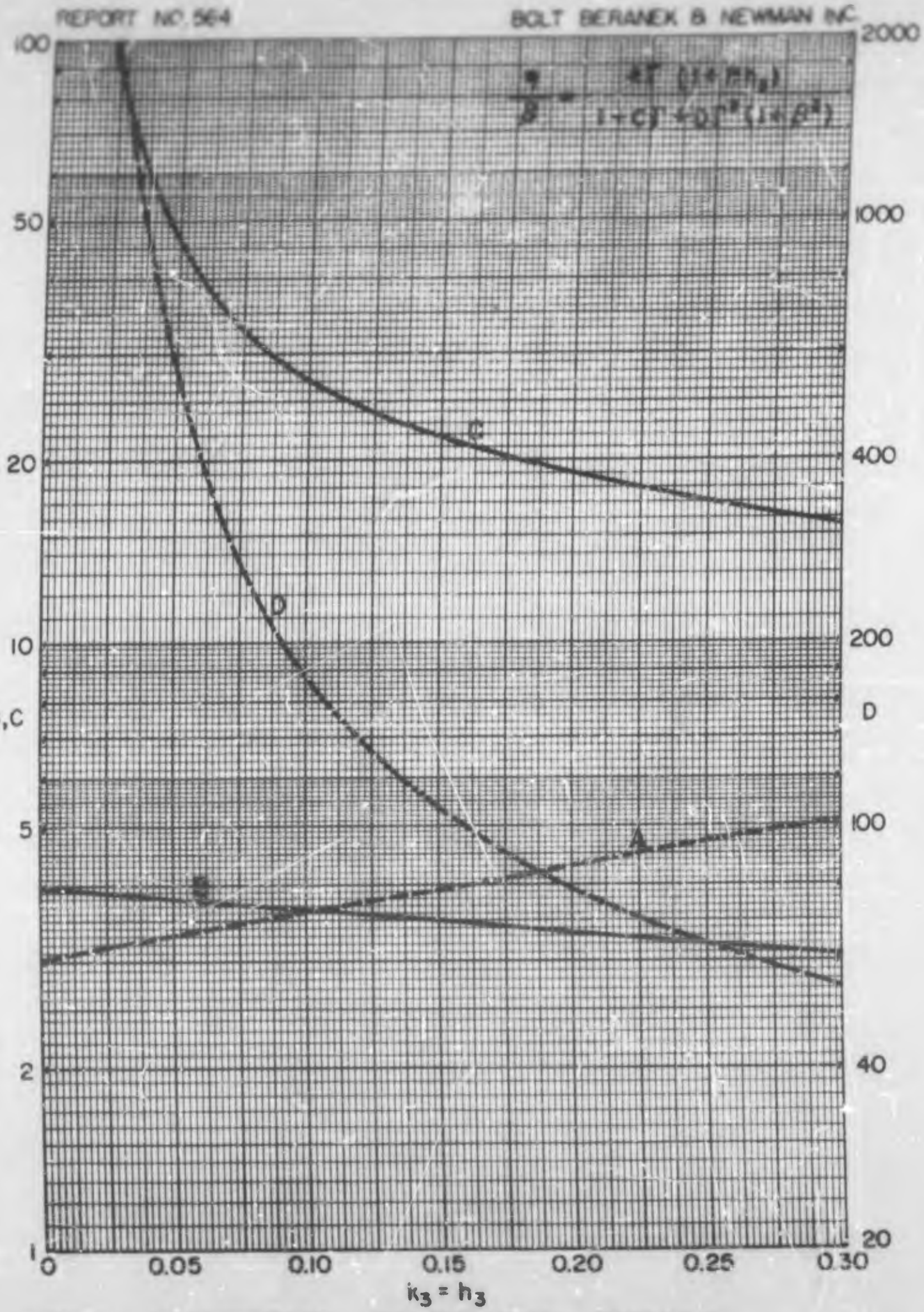

FIG. 12 APPROXIMATE CALCULATION FORMULA FOR CONSTRAINED DAMPING LAYERS ($E_3 = E_1$)

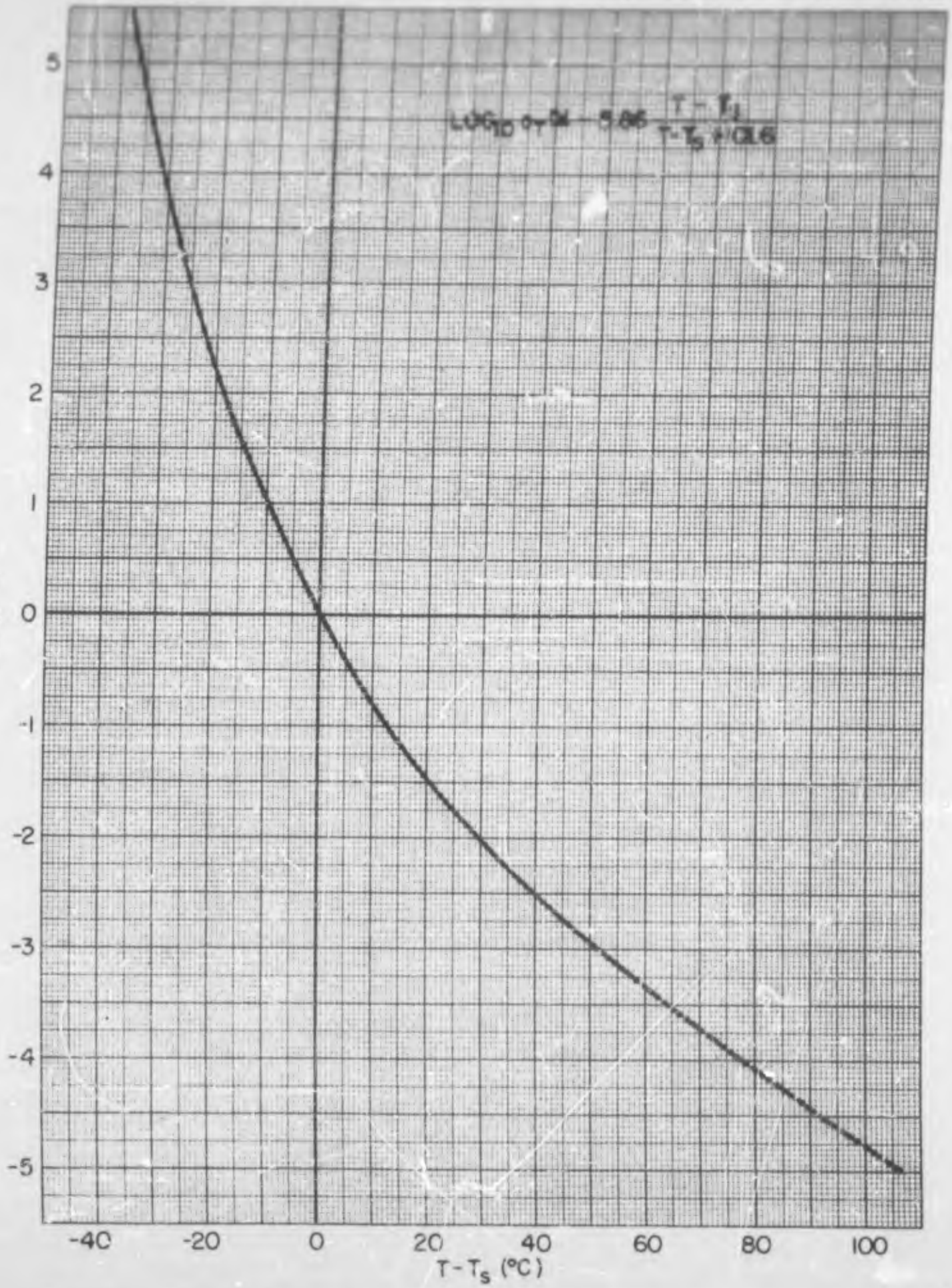

FIG. 13 FUNCTION RELATING TEMPERATURE TO FREQUENCY FOR HIGH POLYMERS. (WILLIAMS, LANDEL, FERRY, J. AM. CHEM. SOC. 77, 3701, 1955)

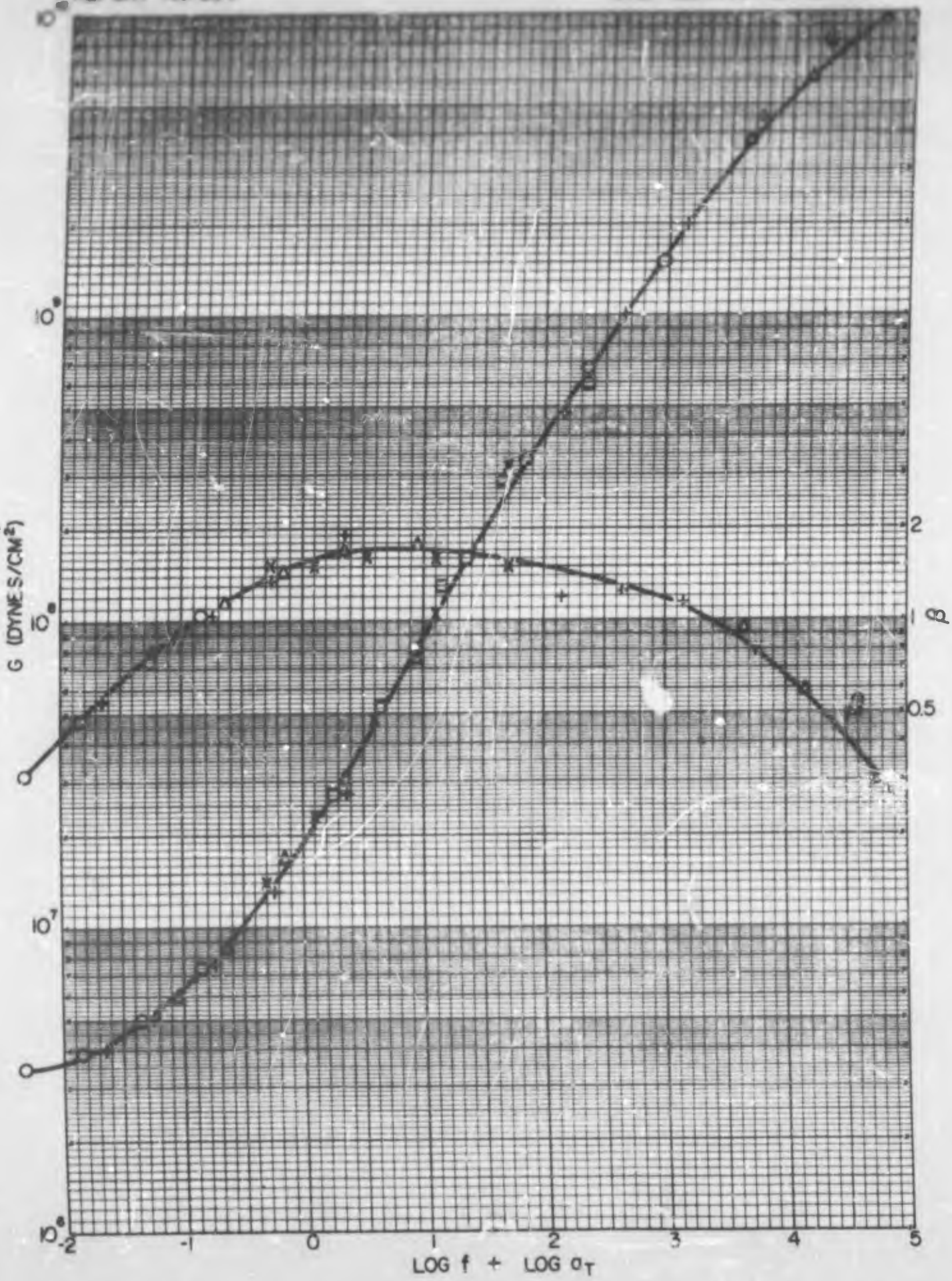

FIG. 14 TEMPERATURE - FREQUENCY CORRELATION OF DYNAMIC SHEAR MODULUS OF POLYISOBUTYLENE.

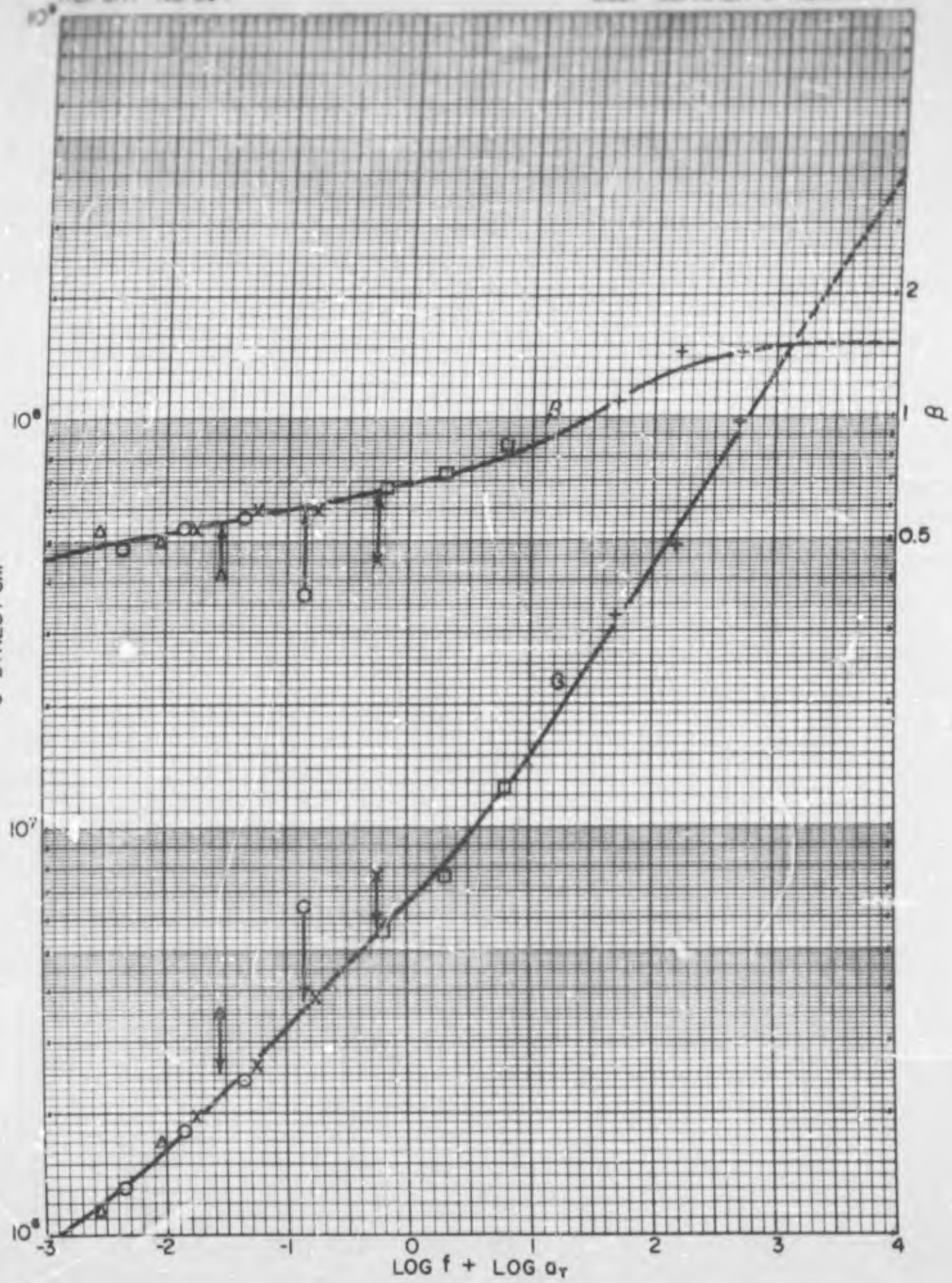

FIG. 15 REDUCED PLOT OF DYNAMIC SHEAR MODULUS DATA FOR 3M ADHESIVE.

AD162382

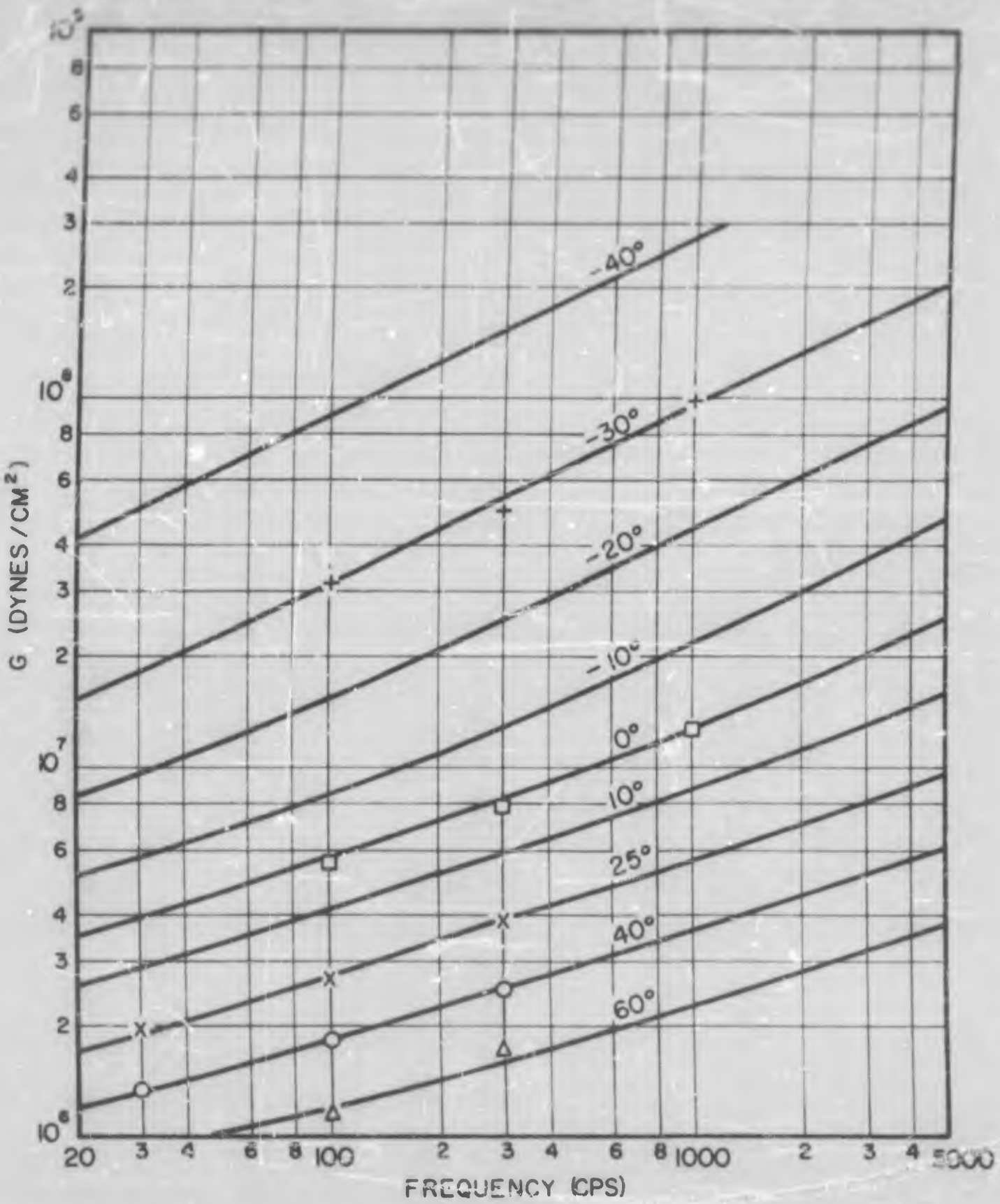

FIG. 16 REAL PART, G, OF SHEAR MODULUS OF 3 M CO. "SOUND DAMPING TAPE" ADHESIVE (DATA POINTS BY MANUFACTURER.)

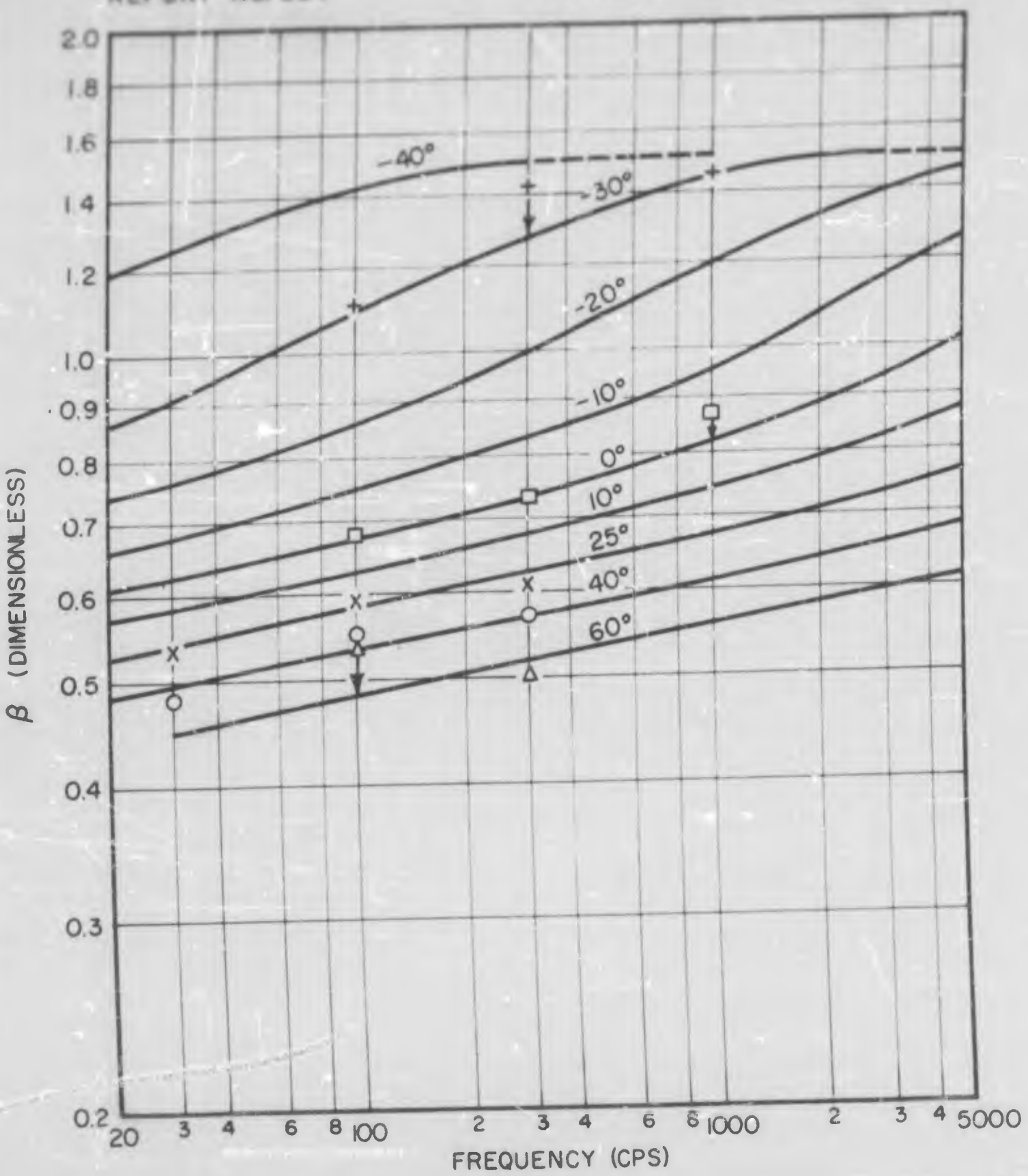

FIG. 17 NORMALIZED IMAGINARY PART, β, OF SHEAR MODULUS OF 3 M CO. "SOUND DAMPING TAPE" ADHESIVE. (DATA POINTS BY MANUFACTURER.)

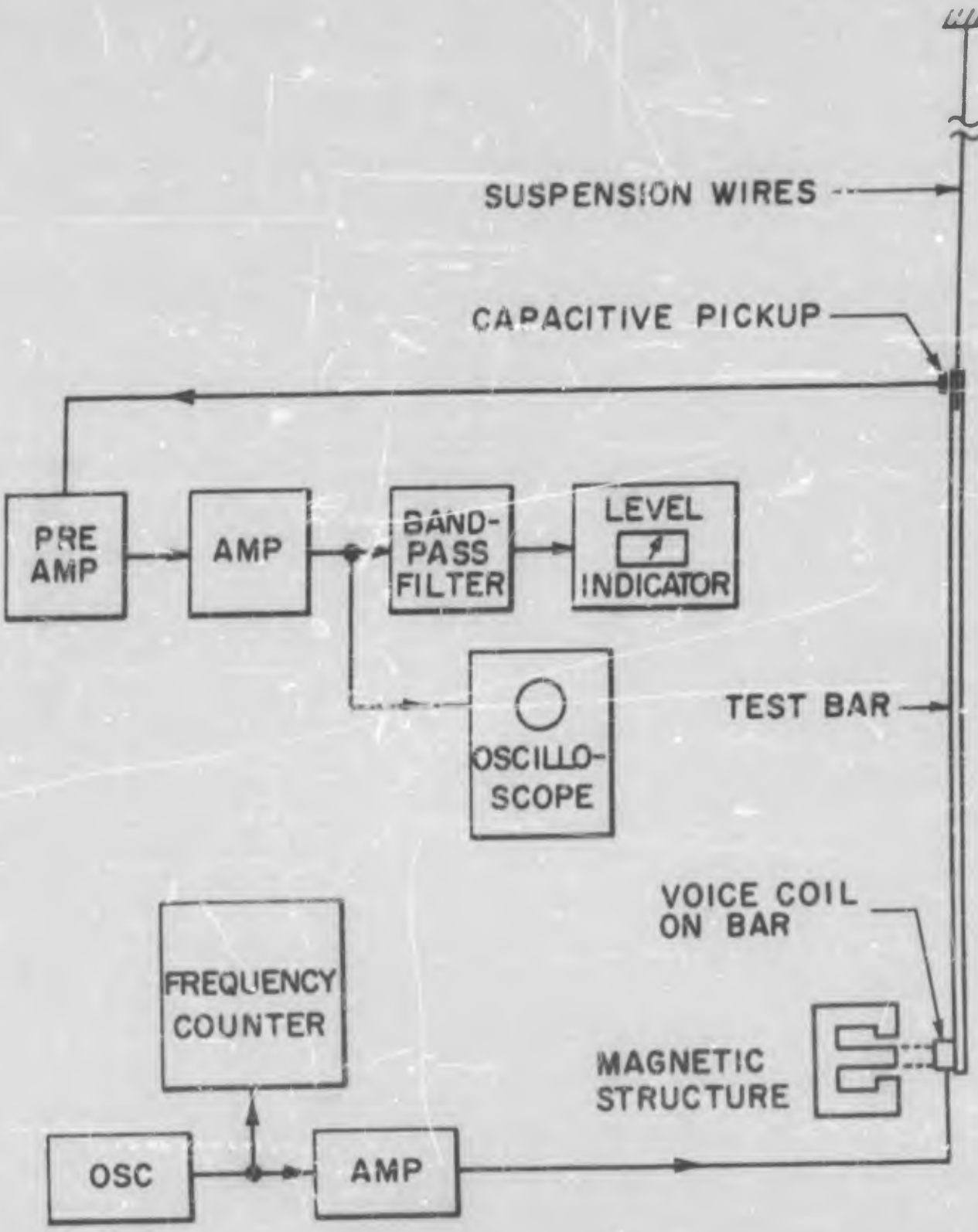

FIG. 18 APPARATUS FOR MEASURING LOSS FACTOR OF TEST BAR BY RESONANCE METHOD.

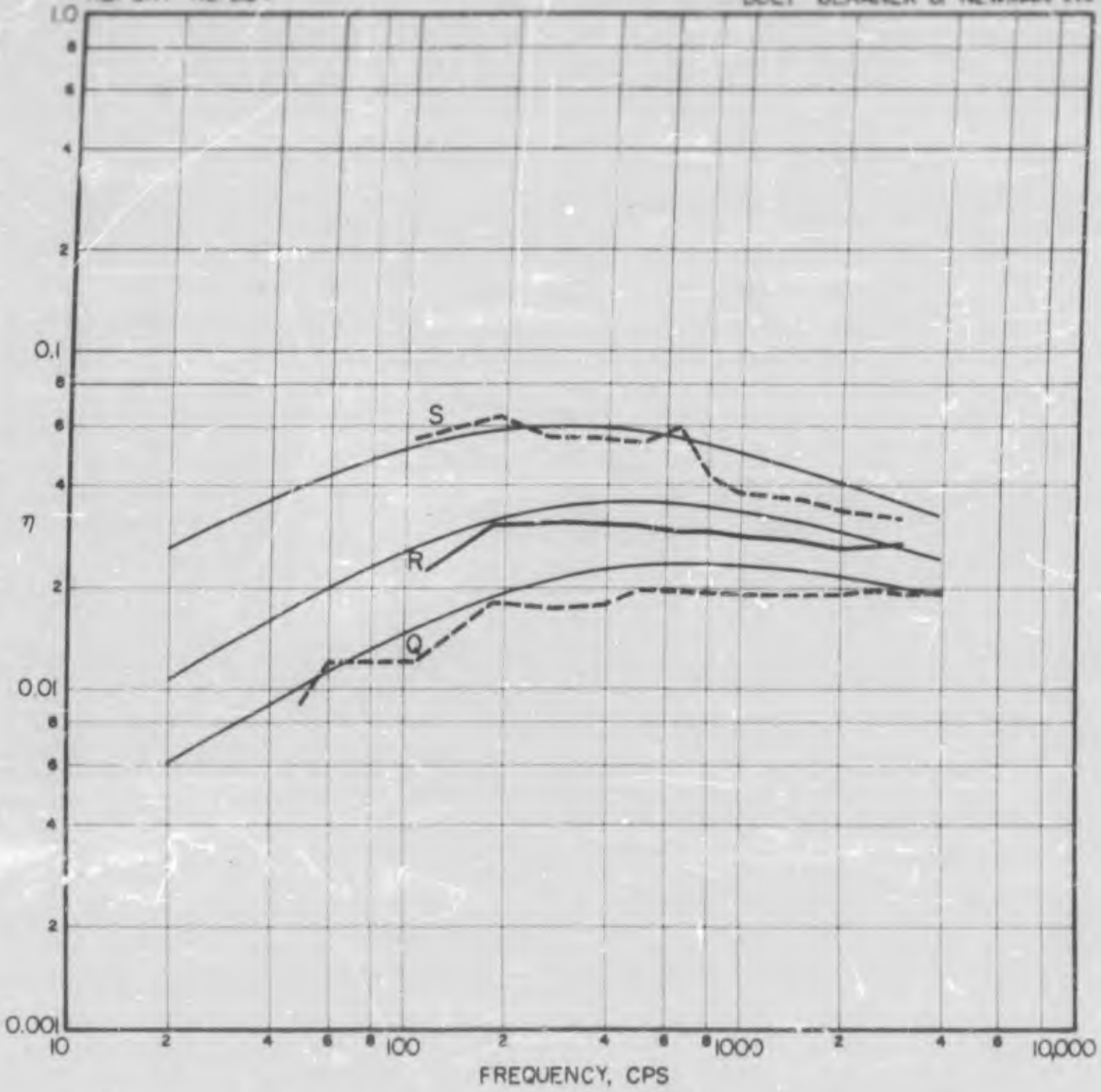

FIG. 19 COMPARISON OF CALCULATED AND EXPERIMENTAL DAMPING FACTORS OF THREE BARS AT ROOM TEMPERATURE.

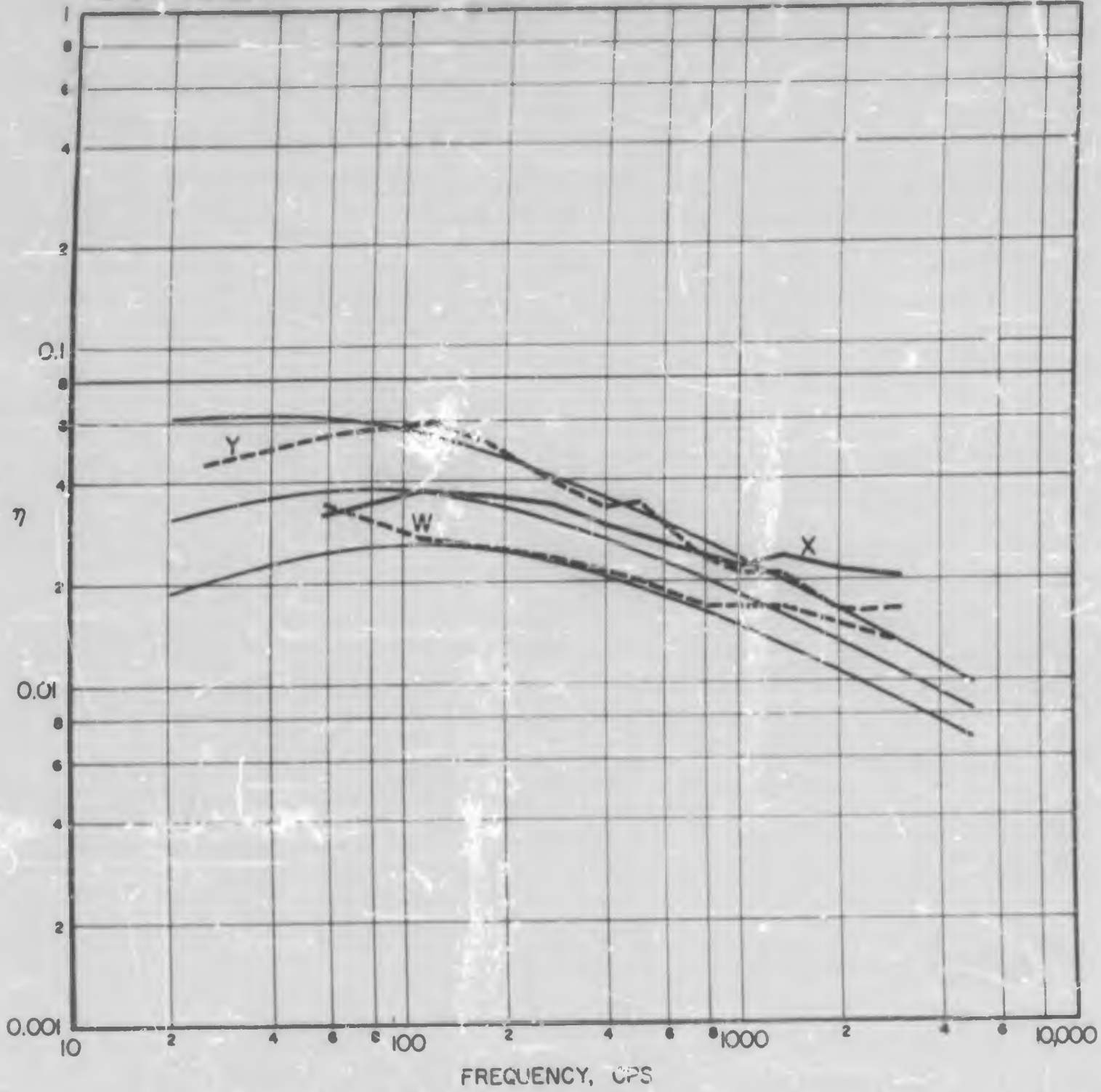

FIG. 20 COMPARISON OF CALCULATED AND EXPERIMENTAL DAMPING FACTOR OF THREE BARS AT ROOM TEMPERATURE.

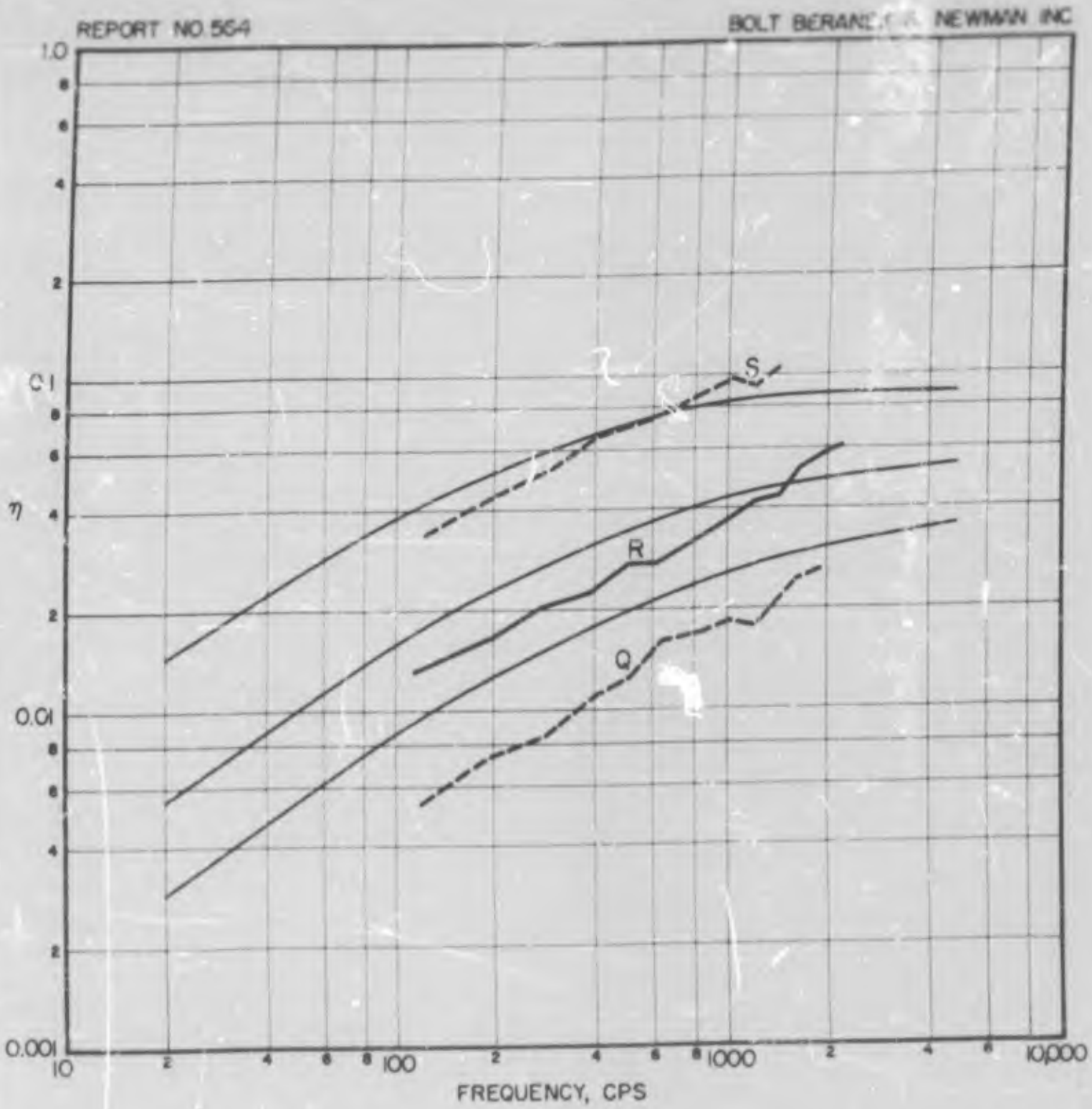

FIG. 21 COMPARISON OF CALCULATED AND EXPERIMENTAL DAMPING FACTORS OF THREE BARS AT -6° C.

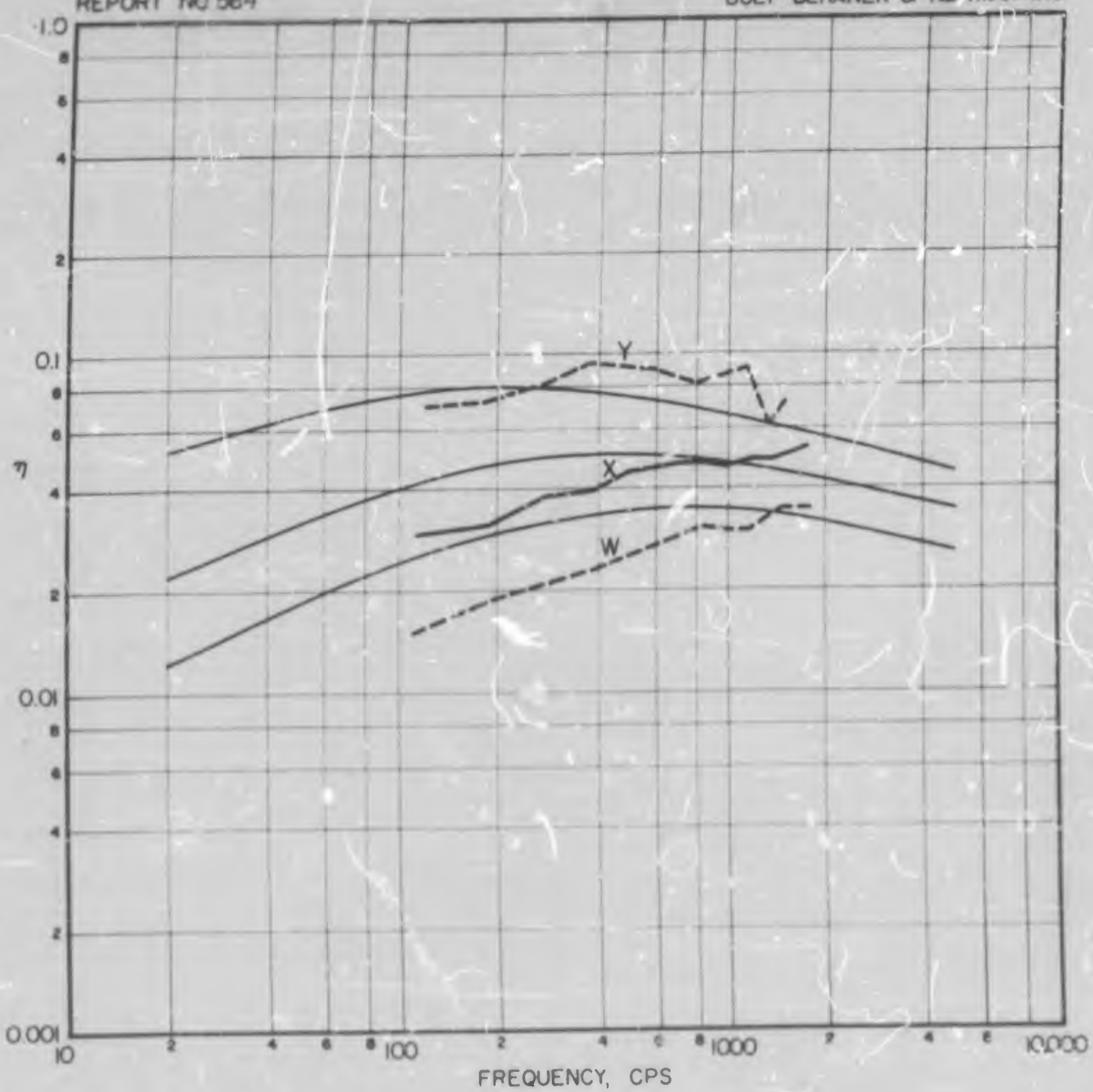

FIG. 22 COMPARISON OF CALCULATED AND EXPERIMENTAL DAMPING FACTORS OF THREE BARS AT -6° C.

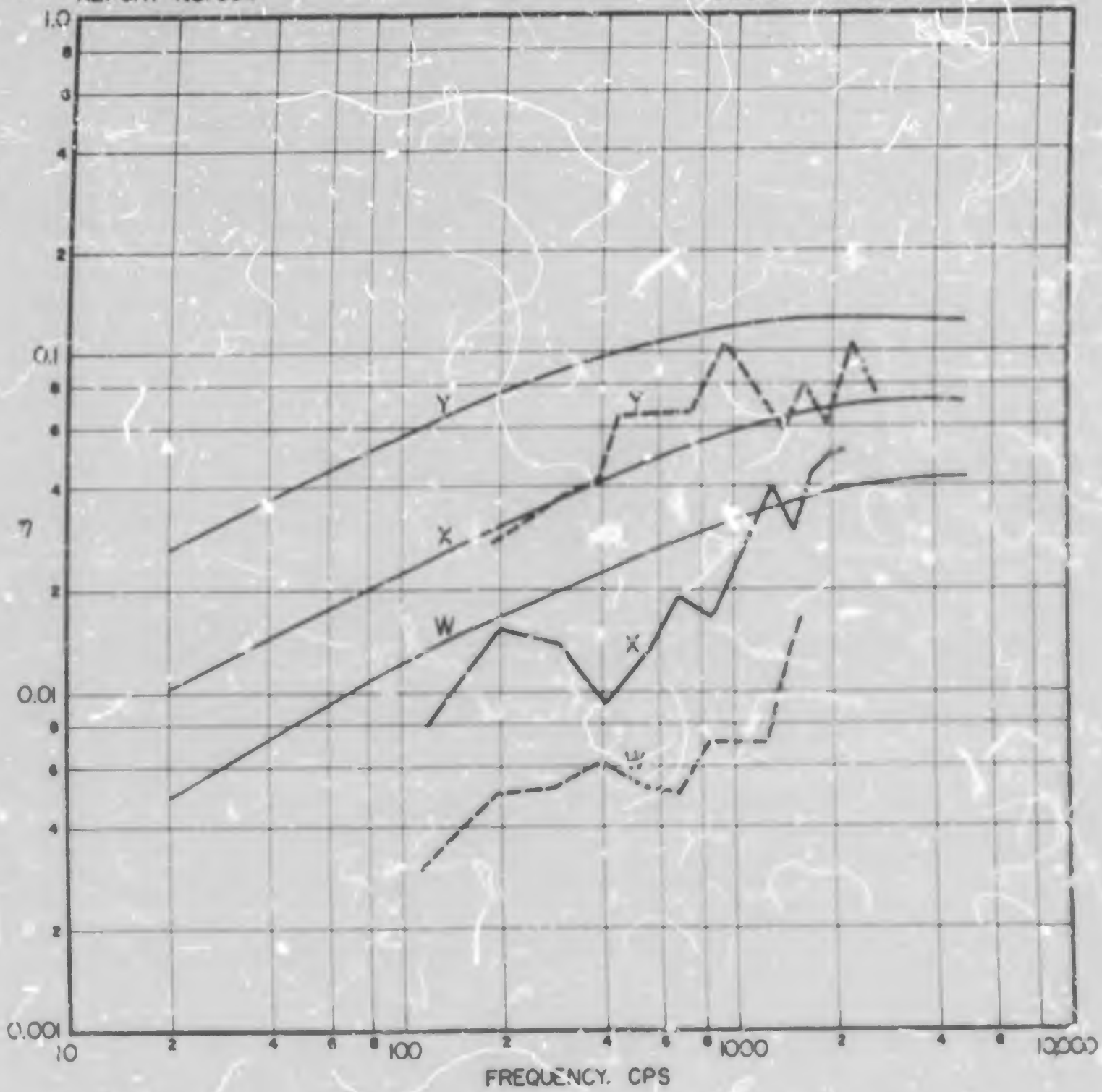

FIG. 23 COMPARISON OF CALCULATED AND EXPERIMENTAL DAMPING FACTORS OF THREE BARS AT -28° C.

AD62382